REGULATION OF PROINFLAMMATORY EXTRACELLULAR VESICLES FROM HIV INFECTED CELLS BY CBD

by

Maria Cowen

A Thesis
Submitted to the
Graduate Faculty
of
George Mason University
in Partial Fulfillment of
The Requirements for the Degree
of
Master of Science
Biology

Committee:

_____	Dr. Fatah Kashanchi, Thesis Chair
_____	Dr. Lance Liotta, Committee Member
_____	Dr. Ramin Hakami, Committee Member
_____	Dr. Iosif Vaisman, Director, School of Systems Biology
_____	Dr. Donna Fox, Associate Dean, Office of Student Affairs & Special Programs, College of Science
_____	Dr. Fernando Wilhelm-Miralles, Dean, College of Science
Date: _____	Fall Semester 2020 George Mason University, Fairfax, VA

Regulation of Proinflammatory Extracellular Vesicles from HIV Infected Cells by CBD

A Thesis submitted in partial fulfillment of the requirements for the degree of Master of Science at George Mason University

by

Maria Cowen
Bachelor of Science
George Mason University, 2019

Director: Fatah Kashanchi, Professor
George Mason University

Fall Semester 2020
George Mason University
Fairfax, VA

DEDICATION

This is dedicated to my parents, family, friends, and coworkers who have supported me throughout this work.

ACKNOWLEDGEMENTS

I would like to thank the many friends, relatives, and supporters who have made this happen. Additionally, I would like to acknowledge and give a special thank Dr. Kashanchi and Gwen Cox, who have taught and guided me.

TABLE OF CONTENTS

LIST OF FIGURES

LIST OF ABBREVIATIONS

Human Immunodeficiency Virus type I HIV-1
Combination Antiretroviral Therapy ..... cART
Food and Drug Administration ..... FDA
HIV-associated Neurocognitive Disorders ..... HAND
Ribonucleic Acid ..... RNA
Trans-activation Response ..... TAR
Extracellular Vesicles ..... EVs
Apoptotic Intrinsic Factors ..... AIFs
Deoxyribonucleic Acid ..... DNA
Central Nervous System ..... CNS
Blood Brain Barrier ..... BBB
Asymptomatic Neurocognitive Impairment ..... ANI
Mild Neurocognitive Disorder ..... MND
HIV-associated Dementia ..... HAD
Cannabidiol ..... CBD
Adenosine Triphosphate ..... ATP
MicroRNA ..... miRNA
Monocyte-derived Macrophages ..... MDMs
Cyclin-dependent Kinases ..... CDKs

ABSTRACT

REGULATION OF PROINFLAMMATORY EXTRACELLULAR VESICLES FROM HIV INFECTED CELLS BY CBD

Maria Cowen, MS

George Mason University, 2020

Thesis Director: Dr. Fatah Kashanchi

As of 2019, approximately 62% of the 37.9 million individuals infected with Human Immunodeficiency Virus type 1 (HIV-1) underwent combination antiretroviral therapy (cART) treatment, which includes a cocktail of inhibitory drugs for nearly all parts of the viral life cycle. The lack of an FDA approved viral transcription inhibitor allows for persistent non-processive transcription which results in the production of short non-coding RNAs (TAR and TAR-*gag*). Our lab and others have shown that these RNAs are released from the cell in extracellular vesicles (EVs), specifically exosomes, and can induce production of proinflammatory cytokines in recipient myeloid cells; a factor that may contribute to the neuroinflammation observed in HIV-1 infected individuals with HIV associated neurocognitive disorder (HAND). Here, we demonstrate that EVs released from HIV-1 infected macrophages with and without cART induce the production of proinflammatory cytokines from astrocytes via activation of TLR3 by EV

cargo (TAR) and have identified three TAR inhibitor candidates to inhibit this mechanism. Furthermore, we show that CBD can lower secretion of EVs and their viral cargo potentially through intracellular viral transcription inhibition. Overall, this study demonstrates the therapeutic potential for CBD usage on lowering EV-mediated neuroinflammation seen in HAND.

INTRODUCTION

As of 2019, approximately 37.9 million individuals were infected with Human Immunodeficiency Virus type 1 (HIV-1) globally with 1.7 million new global cases and 1.1 million infected patients in the United States[3,4]. Of the globally infected patients, 62% had access to and were undergoing combination antiretroviral therapy (cART) treatment, which involves a cocktail of inhibitory drugs for nearly all parts of the viral life cycle including fusion, entry, protease activity, reverse transcriptase activity, integrase activity, and virion assembly[3,5]. Although the invention of cART has led to the increased patient longevity and quality of life, the increased lifespan has resulted in an increase in the appearance of mild symptoms of HIV-1 associated neurocognitive disorders (HAND). This is potentially due persistent viral transcription due to the lack of a HIV-1 transcription inhibitor[6]. In line with this, a study by Hatano et al. showed patients undergoing cART displayed high expression of viral transcripts inside $CD4^+$ T cells, contradictory to the undetectable viral load circulation in the blood[7]. Moreover, Kumar et al., demonstrated that these HIV-1 patients undergoing cART treatment have viral components, specifically viral short non-coding RNAs, accumulating in several different regions of the brain, which may contribute to HAND[8]. Over the past several years, the Kashanchi lab and others have published several studies showing the presence of HIV-1 viral short non-coding and long RNA transcripts, TAR and *env*, in extracellular vesicles (EVs), specifically exosomes,

released from HIV-1 infected cells. Furthermore, we have shown that these exosomes can induce production of pro-inflammatory cytokines in recipient cells[9,10]. Production of pro-inflammatory cytokines have been shown to worsen disease progression, leading to patient symptoms such as inflammation, tissue destruction, and death[11]. Additionally, we have shown that even in infected patients undergoing cART treatment, exosomes carry both TAR and *env* viral RNA transcripts, as well as viral proteins such as p24 and nef, which may potentially contribute to the neurodegeneration seen in HAND[12]. Thus, due to the lack a FDA-approved viral transcription inhibitor, short non-coding RNAs (such as TAR and TAR-*gag*) and genomic RNAs (*env*) are transcribed in the nucleus, exported into the cytoplasm where they will accumulate due a virally mediated autophagy inhibition, resulting in cellular activation of packaging viral RNAs into extracellular vesicles to ship out and rid the cell of viral nucleic acid build up.

EVs are membrane bound vesicles which range from 30 to greater than 1000 nanometers (nm) in size and are involved in cell-to-cell communication. EVs are categorized into different subpopulations, including- from largest to smallest- apoptotic bodies, microvesicles, exosomes, and exomeres, all of which populations differ in function, biogenesis, and composition. Intriguingly, the field of extracellular vesicles is a relatively new field in the scientific community, which results in increased blurredness between distinguished EV populations, especially regarding exomeres. Apoptotic bodies (ranging roughly 1000 nm and greater) are formed after an extracellular or intracellular trigger, such as apoptotic intrinsic factors (AIFs), of the extrinsic or intrinsic apoptotic signal transduction pathway, inducing DNA fragmentation and chromosomal condensation,

which would ultimately result in nuclear blebbing of nucleosomes into secreted vesicles to be engulfed by recipient cells[13]. Biogenesis of microvesicles (ranging from roughly 100 – 1000 nm) includes incorporation of both nucleic acids and proteins by proteins such as ARF6, as well as budding out of vesicles from the cellular plasma lipid bilayer membrane[14,15]. Within the autophagy pathway, a cellular mechanism for lysosomal degradation of nutrients such as proteins, includes a secretory autophagic component allowing the release of autophagosomes into the extracellular environment to be incorporated by neighboring cells or engulfed via phagocytosis by macrophages; often secreted autophagosomes are included in the microvesicular EV population[16]. Similarly to microvesicles, exosomes (ranging 30-100 nm),incorporate nucleic acids and proteins into vesicles, however, are formed and released through invagination of multivesicular bodies in late endosomal vesicles via the endosomal complexes required for transport (ESCRT) dependent and independent pathways[17]. Exomeres (ranging less than 30 nm), newest of the emerging EV field, have entirely unknown biogenesis and thus methods of isolation are still being pursued[18]. For analytical purposes, the standardization of isolation techniques of these different EV populations has become critical in the EV field to provide a better method for characterization of separate populations. The most standardized and well accepted method across the EV field involves a series of differential ultracentrifugations at 2,000 *x g* (or 2K) to pellet the apoptotic bodies, 10,000 *x g* (or 10K) to pellet the microvesicles, and 100,000 *x g* (or 100K) to pellet the exosomes from cell culture supernatant. As EVs are involved in intracellular communication, different EV populations have been implicated in disease pathogenesis for cancer and infectious disease, as studies

have demonstrated the implications of EVs in disease-related neurocognitive disorders[19–21].

The central nervous system (CNS) is comprised of a heterogenous population of cells such as astrocytes (which make up the majority), neurons, microglia, and oligodendrocytes, which all vastly differ in structure and functionality, such as making up and regulating the blood brain barrier (BBB), transmitting neurotransmitters through electrochemical synapses, regulating the immune response via phagocytosis, and providing protection of the neuronal axon sheath, respecitively[22–24]. In terms of neuronal disorders, such as Alzheimer's and Multiple Sclerosis, altered phenotypes are generally present which can include neuronal degradation, de-myelination, and dysfunctional astrocytes, which may may result from neuroinflammation caused by pro-inflammatory signals, such as reactive oxygen and nitrogen species, and pro-inflammatory cytokines[22]. Astrocytes, as regulators and barriers of the CNS, are responsible for regulating pro-inflammatory markers or agents that can cause damage or induce neuronal inflammation, which can result in a change in morphological and functional astrocyte states such as astrogliosis, or reactive astrocytes, or senescent astrocytes[25]. Reactive astrocytes often produce astrocyte scars to increase barrier resistance, but can also, when continually exposed to CNS insults, contribute to neuronal degeneration[26]. Astrocyte senescence, or cellular aging, has also been shown to contribute to neurodegeneration through mechanisms independent of astrogliosis[27]. Additionally, other immune cells such as T lymphocytes and macrophages can traverse through the BBB and can potentially contribute to the secretion of pro-inflammatory cytokines[28]. In terms of HIV-1 infection and HAND, patients diagnosed with

HAND exhibit a range of symptoms including low, mild, and severe amount of neurological impairment for daily functions, ie. motor skills, memory and speech, which are categorized into asymptomatic neurocognitive impairment (ANI), mild neurocognitive disorder (MND), and HIV-associated dementia (HAD)[29]. Although cART treatment lowers circulating virus, ultimately leading to decreased expression of HAD phenotypes in HIV-1 patients, there is increased presence of the milder ANI and MND phenotypes of HAND, with up to 69% of HIV-1 patients exhibiting mild HAND phenotypes[30]. Knowing that the CNS is susceptible to pro-inflammatory damage, potentially from EVs released from infected cells, that can result in lowered functionality in patient daily life and that cART has not been shown to fully inhibit this neuro-inflammation, it is important to characterize and mitigate these symptoms seen in HAND patients.

Cannabidiol (CBD) is a non-psychoactive chemical component isolated from the *Cannabis sativa* plant. Its anti-inflammatory properties has led to FDA-approval of purified CBD, Epidolex, to treat two epileptic disorders called Lennox-Gastaut syndrome and Dravet syndrome, for the purpose of seizure prevention[31]. One rat model study has shown that CBD, having lowered epileptic seizures, induced increased production of early autophagic complexes, which are involved in autophagosome formation[32]. Although few studies have been conducted for analyzing the effect of CBD on HIV-mitigated inflammation, several studies have been done in relation to cancer. EVs, specifically the exosome and microvesicles populations, released from prostate, liver, glioblastoma and breast cancers are reduced upon treatment with CBD[33,34]. Mitochondrial regulation of ATP production is a major biomarker in astrocyte dysfunction, and if CBD-mitigated reduction

in ATP is translational towards astrocytes, CBD treatment may lower astrocyte dysfunction and neuronal degeneration. Interestingly in the case of CBD effect on glioblastomal EVs, CBD was shown not only to lower specific microvesicular subpopulation of EVs, but to also lower the oncogenic miRNA, miR21, cargo content, while increasing the anti-oncogenic miRNAs, miR126, cargo[34].

Taken together, this highlights a gap of knowledge in the field, which involves both the lack of a transcription inhibitor and the lack of an inhibitor targeting EVs carrying viral cargo, potentially contributing to HAND. Therefore, we hypothesize that cannabidiol could be used to mitigate the inflammatory effects on astrocytes by EVs released from HIV-1 infected cells.

MATERIALS AND METHODS

Cell Culture and Reagents

U1 (HIV-1-infected promonocytic), U937 (uninfected promonocyte), CCF-STTG1 (uninfected astrocyte), PBMC (peripheral blood mononuclear) cells were cultured in complete RPMI 1640 media with 10% fetal bovine serum (FBS), 1% L-glutamine, and 1% penicillin/streptomycin (Quality Biological) and incubated in 5% CO2 at 37 °C). Phorbol 12-Myristate 13-Acetate (PMA; 100 nM) was used to differentiate monocytes into monocyte-derived macrophages (MDMs) for 5 days. All cells were incubated at 37°C with 5% CO_2 infusion. U937 and U1 cells were treated with antiretroviral drugs, such as Darunavir, Ritonavir, Emtricitabine and Tenofovir, for 5 days at indicated concentrations. The U937 and U1 cells, as well as the antiretroviral drugs, were provided by the AIDS Reagent Program (National Institutes of Health or NIH). CCF-STTG1 and U138 MG cells were obtained from American Type Culture Collection (ATCC). CCF-STTG1 cells were treated with the indicated concentrations of TAR inhibitor molecules (101FA, 102FA-2, 103FA-2, 104FA-2, 105FA, 106FA-2, 107FA, 108FA, 109FA, 110FA, 111FA, 112FA, 113FA, 115FA, 116FA-2, 120FA, Ral HCl; provided by Dr. Stuart LeGrice in the National Cancer Institute of the NIH) for 3 days. U1 and U1 MDM cells were treated with varying concentrations of Cannabidiol (2-[1R-3-methyl-6R-(1-methylethenyl)-2-cyclohexen-1-yl]-5-pentyl-1,3-benzenediol; Cayman chemicals Cat. #90080). Peripheral blood mononuclear cells (PBMCs) were treated with PHA and IL-2 every other day for a 7 days, followed by infection with HIV-1 89.6 strain and re-treatment with PHA and IL-2. PBMCs

were differentiated into primary macrophages using 100 nM PMA for 5 days, followed by treatment with a titration of CBD.

Ultracentrifugation

Infected MDMs (from 1×10^6 cells per mL culture for 5 days) were cultured in 100 mL RPMI media with 1% L-glutamine, 1% penicillin/streptomycin and 10% exosome-free FBS per sample. The cells were pelleted via centrifugation at 2,000 × *g* for 5 min. The supernatant was ultracentrifuged at 10,000 × *g* for 30 min at 4 °C, where cellular debris was discarded. The supernatant was ultracentrifuged twice more at 100,000 × *g* for 90 min at 4°C, where EVs were pelleted and washed with PBS. The pellets were resuspended in PBS and used to assess particle concentration and size via Nanoparticle Tracking Analysis (NTA).

ZetaView NTA

To assess for EV concentration and size, Nanoparticle Tracking Analysis (NTA) was used via ZetaView Z-NTA (Particle Metrix; software: ZetaView 8.04.02). The ZetaView was calibrated using 100 nm polystyrene nanostandard particles (Applied Microspheres), where the sensitivity and minimum brightness setting read 65 and 20, respectively. The pre-acquisition parameters for each sample read 23°C for temperature, 85 for sensitivity, 30 frames per second (fps) for frame rate and 250 for shutter speed. One milliliter of diluted EV sample in deionized water was loaded in the cell. The average

diameter size and concentration of the EVs was calculated and analyzed using ZetaView 8.04.02 and Microsoft Excel 2016 (v.15.0.4849.1003).

Cell Viability

MDM, CCF-STTG1, U138, and U1 cells (at 5×10^4 per well) were plated in a 96-well plate. Each sample was plated in triplicate and cell-free media was used for background measurements. The cells were treated with their respective treatments and incubated for either 1, 3, or 5 days, as indicated in the figure legends. CellTiter-Glo reagent Luminescence Viability kit (Promega) and the GLOMAX Multidetection System (Promega) were used to measure luminescence and assess for cell viability. Two plate readings were taken and averages of both readings were calculated.

Preparation of Whole Cell Extracts

Uninfected and infected monocytes and macrophages were centrifuged at 15,000 × *g* at room temperature for 5 minutes, producing a cell pellet and supernatant. The cell pellets were washed with 1x Phosphate Buffer Saline (PBS) without Calcium and Magnesium and resuspended in lysis buffer, which includes: 120 mM sodium chloride (NaCl), 50 mM Tris-hydrochloric acid (HCl)- pH 7.5, 50 mM sodium fluoride (NaF), 5 mM Ethylenediaminetetraacetic acid (EDTA), 0.5% Nonidet P-40 (NP40), 0.2 mM sodium orthovanadate (Na_3VO_4), 1 mM Dithiothreitol (DTT), and 1 complete protease inhibitor cocktail tablet/50 mL (Roche Applied Science, Mannheim, Germany). The pellets were incubated on ice for 20 min whilst vortexing every 5 minutes. The whole cell lysate

supernatants were separated from cell debris through centrifugation at 10,000 × *g* at 4 °C for 10 minutes. Bradford assay (Bio-Rad) was used to determine the protein concentration according to the manufacturer's protocol.

Enrichment of EVs with Nanotrap Particles

Nanotrap (NT) particles (Ceres Nanosciences) were used to enrich for EVs in relatively low volumes. A three-equal-part slurry of NT80 particles (Ceres #CN1030), NT82 particles (Ceres #CN2010), and PBS was mixed as described previously[12]. The supernatants were nanotrapped with NT80/82 (30 uL beads/mL supernatant) and rotated overnight at 4°C. The NT80/82 particles were pelleted at 15,000 × *g* at room temperature for 5 minutes and washed with PBS.

Western Blot

For Western blot assays, Laemmli buffer (Tris Glycine SDS and β-mercapomethanol) was added to whole cell lysate samples and NT pellet samples. Samples were heated at 95 °C for 3 minutes. Samples were loaded into 4-20% Tris-glycine gels (Invitrogen) with a Precision Plus Protein™ Standard (BioRad) and gel electrophoresis was run at 150 V until completion. The gels were transferred onto Immobilon Polyvinylidene fluoride (PVDF) membranes (Millipore) at 50 milliamps overnight. Five percent milk in PBS containing 0.1% Tween-20 (PBS-T) was used to block the protein membranes for 2 hours at 4°C. Primary antibody in PBS-T was added to the membranes to incubate overnight at 4°C; primary antibodies include: α-p24 (Cat: 4121, NIH AIDS

Reagent Program), α-Nef (Cat: 3689; NIH AIDS Reagent Program), α-gp120 (Cat: 522; NIH AIDS Reagent Program), α-CD81 (Cat: EXOAB-CD81A-1; SBI), α-VPS4 (Cat: sc-32922; Santa Cruz Biotechnology), α-CHMP6 (Cat: sc-67231; Santa Cruz Biotechnology), and α-Actin (ab-49900), as well as senescence antibodies such as p21/Waf1, p16, p-H2AX, Lamin B1, IL-6, MMP-3, and HMGB1 from the Senescence Marker Antibody Sampler Kit (Cat: 56062T; Cell Signaling Technology), TLR3 (Cat: 6961S; Cell Signaling Technology) and reactive gliosis marker GFAP (Cat: sc-33673; Santa Cruz Biotechnology). The membranes were washed three times with PBS-T for 5 minutes per wash. Complementary HRP-conjugated secondary antibodies were added to the membranes and incubated for 2 hours at 4°C. The membranes were washed two times with PBS-T and one time with PBS, 5 minutes per wash. HRP luminescence was activated with Clarity Western ECL Substrate (Bio-Rad). The membranes were developed using the Molecular Imager ChemiDoc Touch system (Bio-Rad).

Kinase Assay

Purified Src antibody (Cat: sc-19; Santa Cruz Biotechnology; 10 ng), TLR3 antibody (100 ng), TAR RNA (100 ng), and TAR inhibitor drugs (101FA, 102FA-2, 103FA-2, 104FA-2, 105FA, 106FA-2, 107FA, 108FA, 109FA, 110FA, 111FA, 112FA, 113FA, 115FA, 116FA-2, 120FA, Ral HCl; 1 μM) were washed with TNE_{50} buffer (Tris (pH7.5), NaCl, EDTA) and kinase buffer, followed by 1-hour incubation period at 37°C with γ-^{32}P ATP and purified histone H1. The samples (50%) were loaded and run through SDS-PAGE on a 4-20% Tris-Glycine gel, followed by staining with Coomassie blue,

destained with destain buffer, and a 2-hour drying period. The dried gels were exposed to a PhosphorImager Cassette, followed by analysis via Molecular Dynamic's ImageQuant Software.

Densitometry Analysis

Densitometry analysis was performed using ImageJ software. Densitometry data were normalized using a two-stop process to control for both exposure and loading. First, background measurements for each membrane were subtracted from the measurement of interest. Next, each protein band was normalized to the corresponding Actin. The normalized counts are represented as an increase or decrease relative to the untreated control (lane 1 set to 100%). Reduction trends were calculated by subtracting the normalized treated lane counts from the normalized control lane counts.

RNA Isolation, Reverse Transcription, and Quantitative Polymerase Chain Reaction (RT-qPCR)

For the isolation of total RNA from cell pellets, cells were harvested, washed once in 1x PBS without Calcium and Magnesium and resuspended in 50 µL of 1x PBS without Calcium and Magnesium. For the isolation of total RNA from EVs, Nanotrap particles were incubated and harvested as described above, then resuspended in 50 µL of 1x PBS without Calcium and Magnesium. Total RNA was isolated from cell pellets and NT80/82 pellets bound with EVs using Trizol Reagent (Invitrogen) as described by the manufacturer's protocol. cDNA was generated using GoScript Reverse Transcription

Systems (Promega) using Envelope Reverse: (5′-TGG GAT AAG GGT CTG AAA CG-3′; Tm = 58 °C), and TAR Reverse: (5′-CAA CAG ACG GGC ACA CAC TAC-3′, Tm = 58 °C) primers. Serial dilutions of DNA from a CEM T-cell line containing a single copy of HIV-1 LAV provirus per cell (8E5 cells) were used as the quantitative standards. RT-qPCR conditions were as follows: one cycle for 2 minutes at 95 °C, followed by 41 cycles of 95 °C for 15 seconds and 58 °C for 40 seconds. Reactions were performed in triplicate using the BioRad CFX96 Real Time System. Quantitation was determined using cycle threshold (Ct) values relative to the 8E5 standard curve using the BioRad CFX Manager Software. Analysis of generated raw data was analyzed using Microsoft Excel 2016.

Statistical Analysis

Standard deviations were analyzed using Microsoft Excel software for quantitative experiments. Two-tailed Student's *t*-test was used to calculate *p*-values, where analysis was determined statistically significant when * = $p < 0.05$, ** = $p < 0.01$, and *** = $p < 0.001$.

RESULTS

cART increases release of EVs secreted from HIV-1 infected monocytes

Since our lab and others have previously shown that EVs released from HIV-1 infected cells carry high amounts of viral RNAs, such as TAR RNA, despite antiretroviral therapy treatment, we decided to further investigate the role of these EVs in HAND[12]. To pursue this, we first sought to confirm that the administration of cART drugs, which are recommended for the treatment of HIV-1 in individuals with CNS infection, could elicit an increase in the release of EVs from infected myeloid cells. U1 and U937 were treated for 5 days with Darunavir, Ritonavir, Emtricitabine, Tenofovir, or a combination thereof and resulting supernatants were analyzed via Nanotracking analysis (NTA; **Fig. 1**). Data in **Fig. 1A** demonstrates that Ritonavir (lane 3), Tenofovir (lane 6), and to a lesser extent Darunavir (lane 2) alone, caused a statistically significant increase in EV release from HIV-1 infected cells (58%, 31%, and 11% increase, respectively). Furthermore, when all four cART drugs were used in combination, as would be used in the treatment of patients, there was a 45% increase in EV release (lane 7), suggesting this recommended regimen could potentially contribute to chronic inflammation in cART treated patients. Conversely, in the absence of HIV-1 infection, Darunavir (lane 2), Ritonavir (lane 3), and Tenofovir (lane 6) alone decreased EV production (**Fig. 1B**). However, similar to U1, treatment of U937 cells with a combination of drugs (lane 7) increased EV release by 69%, potentially contributing to reactivation of the latent viral reservoir[1,35].

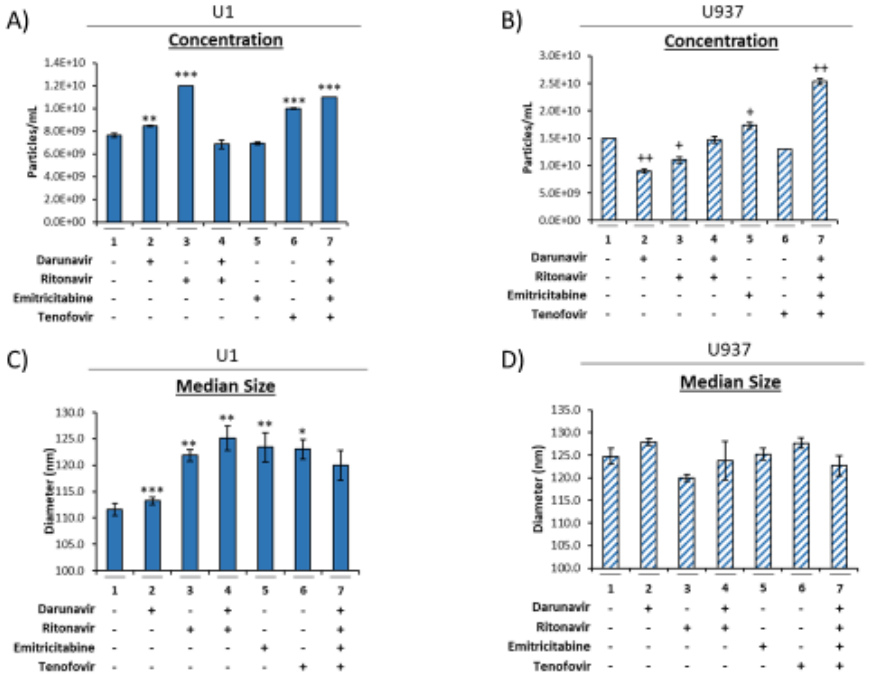

Figure 1. Antiretrovirals increase the release of EVs from HIV-1 infected monocytes. U1 (HIV-1 infected monocytes) and U937 (uninfected monocytes) cells were treated twice with Darunavir (10 µM), Ritonavir (5 µM), Darunavir/Ritonavir (10 µM/ 5 µM), Emtricitabine (10 µM), Tenofovir (10 µM), or a combined regimen for 5 days in exosome-free media. Supernatants were analyzed using NTA to assess for drug mediated changes in released EV numbers in treated U1 (**A**) and U937 (**B**) cells. Additional analysis investigated change in EV median diameter from U1 (**C**) and U937 (**D**) cells. Statistical significance was assess using a Student's t-test comparing treated samples (lanes 2-7) to untreated control (lane 1). $*p < 0.05$, $**p < 0.01$, $***p < 0.001$.

The results in **Fig. 1C** show an increase in the median diameter size of EVs released from HIV-1 infected monocytes following treatment with every tested cART drug (lanes 2-7) and a significant increase when treated with Ritonavir (lane 3), Darunavir/Ritonavir (lane 4), Emtricitabine (lane 5), Tenofovir (lane 6), and a combination (lane 7). However, in the treatment of uninfected U937 cells, cART did not cause a significant change in the mean diameter of released EVs (**Fig. 1D**). Overall, these findings suggest there may be an increase in the release of larger vesicles from HIV-1 infected monocytes post-cART while EVs released from uninfected cells maintain their EV size distribution.

EVs released from HIV-1 infected monocyte-derived macrophages (MDMs) induce intracellular changes in astrocytes

As HAND poses a threat to the quality of life of adequately suppressed HIV-1 patients, we next wanted to evaluate the role EVs had from infected macrophages on recipient CNS cells, specifically astrocytes. As we have previously shown that EVs released from infected cells can cause an increase in the production of proinflammatory cytokines in uninfected recipient cells[10] and that these EVs can be found within the CSF of individuals infected with HIV-1[36], we hypothesized that treatment with infected macrophage-derived EVs could elicit changes in astrocytes. To test this, U1 HIV-1 infected monocytes were differentiated into macrophages using PMA and treated twice with cART (10 μM; Darunavir, Ritonavir, Tenofovir, and Emtricitabine) for 5 days. Donor cell viability was assessed to determine optimal drug concentrations (data not shown**).** Following incubation, total EVs were isolated using ultracentrifugation and EV

concentration was normalized to control numbers (**Fig. 2A**). These EVs were used to optimize EV treatment of two astrocyte cell lines, CCF-STTG1 and U138, at a 1:10,000 ratio of cell:EVs over the course of either 1, 3 and 5 days for cell viability assessment. These data demonstrated that both EV treatments from HIV-1 infected MDMs with and without cART treatment resulted in lowered ATP production and, thus, lowered astrocyte proliferation (**Fig. 2B**). The data also showed all three incubation periods resulted in lowered astrocyte proliferation, with the latter two being the most statistically significant. Therefore, 3- day incubation periods on astrocytes were used for the remaining experiments because it demonstrated lowered, yet intermediate decline in cell death.

Astrocytes have been shown to respond to injury and infection by inducing phenotypic and functional changes to enter an activated state or a senescent state. The former is termed reactive astrogliosis, by which the intracellular rise of calcium influx causes the astrocytes to be activated and undergo glial scar formation for reparation of injury and neuroprotection[37,38]. To further assess for changes in astrocyte functionality, senescence markers and astrogliosis markers were examined upon EV treatment. EVs released from U1 MDMs that were treated with cART were treated on astrocytes (CCF-STTG1 and U138) at a 1:10,000 ratio for 3 days. Cells were lysed and used for Western blot analysis of senescence (cell cycle regulators, nuclear damage, and secreted inflammatory markers) and astrogliosis markers. The results in **Fig. 3A** show in a reduction in the presence of p21/Waf1, a cell cycle regulator, in both CCF-STTG1 (48% reduction, lane 1 *vs*. 2) and U138 cells (28% reduction, lane 3 *vs*. 4) as determined by densitometry analysis (data not shown). The decrease in p21/Waf1 upon treatment suggests a reduction

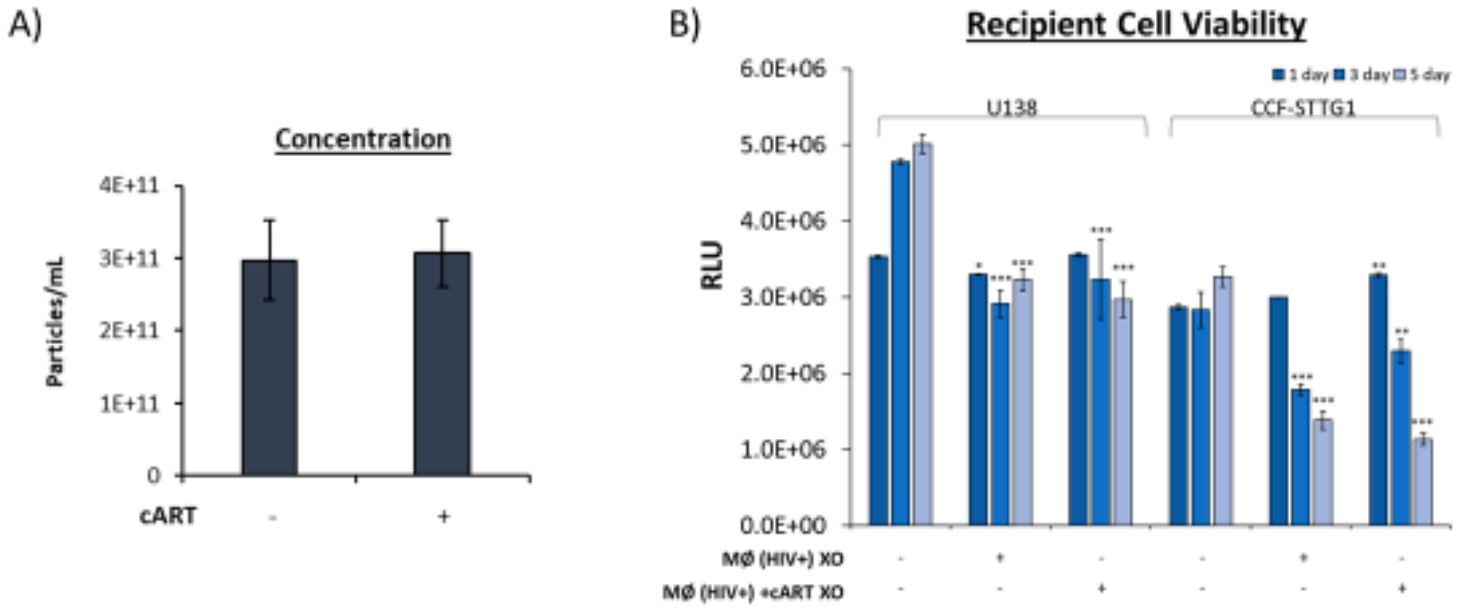

Figure 2. EVs from HIV-1 infected MDMs downregulate astrocyte ATP. A) U1 cells were differentiated into macrophages using PMA and treated with cART (10 μM; Emtricitabine, Tenofovir, Darunavir, and 5 μM Ritonavir) for 5 days. EVs were isolated using ultracentrifugation and assessed for concentration and particle size using ZetaView. T-statistical analysis was taken and was non-significant. **B**) EVs from panel A were treated onto U138 and CCF-STTG1 cells at a 1:10,000 concentration (cell/EV ratio). Viability assays were taken at 1, 3, and 5 days post-treatment. Statistical significance was assess using a Student's t-test comparing treated samples (lanes 2-3, 5-6) to untreated control (lane 1 and 4). $*p < 0.05$, $**p < 0.01$, $***p < 0.001$.

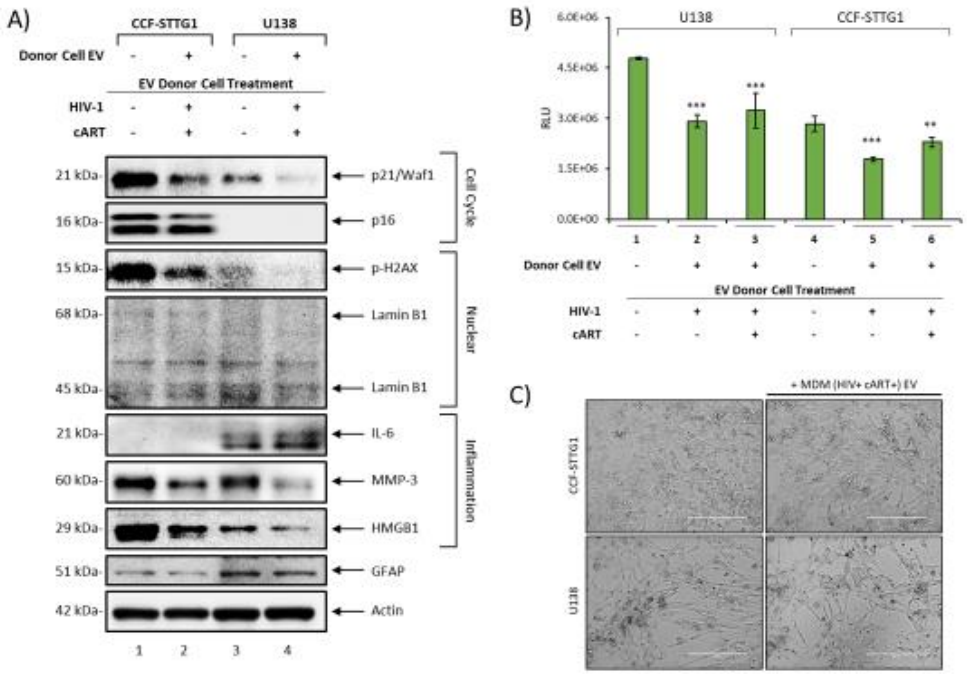

Figure 3. EVs from HIV-1 infected MDMs do not induce senescence or reactive astrogliosis. U1 cells were cultured for 5 days. U1 monocytes were differentiated into MDMs using PMA (100 µM) and treated with ± cART cocktail (10 µM; Darunavir, Emtricitabine, Tenofovir, and 5 µM Ritonavir) for 5 days. **A**) EVs were treated at a 1:10,000 (cell/EV) ratio on CCF-STTG1 and U138 cells (1 x 10^6) for 3 days. Cells were lysed, run through SDS-PAGE, and Western blotted for senescence markers (p21, p16, p-H2AX, Lamin B1, IL-6, MMP-3, and HMGB1), astrogliosis marker (GFAP), and Actin. **B**) EVs were treated at a 1:10,000 (cell/EV) ratio on CCF-STTG1 and U138 cells (5 x 10^4) for 3 days. Cell viability was assessed using Cell-Titer Glo reagent as per manufacturing (Promega) protocol. **C**) Plated cells from panel A were imaged using light microscopy, where scale bar = 200 um. Statistical significance was assess using a Student's t-test comparing treated samples (lanes 2-3, 5-6) to untreated control (lane 1 and 4). $*p < 0.05$, $**p < 0.01$, $***p < 0.001$.

in the inhibition of cyclin-dependent kinases (CDKs) which would, in turn, release cells from arrest, pushing them towards the next stage of cell cycle and eventually increased proliferation[39]. However, Stein et al. has shown the increase in p21 commonly associated with cellular senescence to be a transient phenotype to establish senescence. Furthermore, their data suggests that while elevated p21 is associated with early senescence, the maintenance of senescence is associated with an increase in $p16^{Ink4a}$, a protein which is also involved in cell cycle regulation[40]. Interestingly, p16 levels showed very little change in CCF-STTG1 cells (30% reduction, lane 3 *vs*. 4) and zero presence in both U138 astrocytes samples. These findings suggest that the EV-treated astrocytes are potentially in transition between early senescence and maintained senescence at 3 days post-treatment.

It is well established that the DNA-damage response can result in cell cycle arrest and cellular senescence[41–44]. To determine if the EV-mediate senescent phenotype was initiated by DNA damage we next examined the levels of phosphorylated histone H2A (p-H2AX), a marker of DNA damage. The data in **Fig. 3A** shows a reduction in p-H2AX, by 54% in CCF-STTG1 cells and by 44% in U138 cells compared to the untreated control lanes (data not shown). These data suggest that a DNA-damage-independent mechanism of senescence induction. Alternatively, recent studies have shown that histones can be secreted from the cell in/on EVs or as free protein and can contribute to activation of the innate immune system. Along these lines, a reduction in the presence of p-H2AX within the cell may potentially indicate an additional pathway by which EVs from infected cells can contribute to chronic inflammation by causing the release of extracellular histones[45–48].

The loss of Lamin B1, a nuclear protein involved in regulating nuclear transport as well as chromosomal structure, is a marker of cellular senescence both *in vitro* and *in vivo* and a reduction of Lamin B1 has been associated with chronic neuroinflammatory diseases such as Amyotrophic Lateral Sclerosis[49–52]. The results in **Fig. 3A** show a slight decrease in Lamin B1 (68 kDa) upon EV treatment in CCF-STTG1 (5% reduction, lane 1 *vs*. 2) and in U138 (19% reduction, lane 3 *vs.* 4). Although the reduction in Lamin B1 is minimal, these findings are in line with levels of p21 and p16, suggesting, again, that the treated astrocytes are potentially entering the maintenance stage of senescence. Interestingly, the loss of Lamin B1 has been found to be elicited by activation of p53/RB pathway[49], potentially suggesting a mechanism by which EVs may induce cellular senescence. Additionally, during apoptosis, Lamin B1 can be cleaved by caspases to form cleavage products. The data in **Fig. 3A** shows no change in the 45 kDa Lamin B1 cleavage product in CCF-STTG1 (1 % increase, lane 1 *vs*. 2) and a decrease in Lamin B1 cleavage product in U138 (33% reduction, lane 3 *vs*. 4) suggesting the cells are not undergoing apoptosis.

Finally, cellular senescence is often characterized by an increase in secreted inflammatory markers such as Interleukin 6 (IL-6), matrix metalloproteinase-3 (MMP3), and cytokine high-mobility group protein 1 (HMGB1)[53–56]. The results in **Fig. 3A** show an increase in IL-6 both U138 (12% increase, lane 3 *vs*. 4), indicating an inflammatory state, and an absence of IL-6 in both CCF-STTG1 intracellular samples. Analysis of inflammatory marker matrix metalloproteinase-3 (MMP3) showed decreased levels in CCF-STTG1 (27% reduction, lane 1 *vs*. 2) and in U138 cells (59% reduction, lane 1 *vs*. 2). A similar trend was observed for high-mobility group protein 1 (HMGB1) which decreased

in CCF-STTG1 (56% reduction, lane 1 *vs*. 2) and in U138 cells (17% reduction, lane 3 *vs*. 4). The intracellular decrease in both MMP3 and HMGB1 in EV-treated astrocytes suggests an increase in the release of these products into the extracellular space. Interestingly, the same trend was not observed for IL-6 potentially suggesting that secretion of MMP3 and HMGB1 could be associated with early senescence induction while secretion of IL-6 may be indicative of a maintained senescent state.

As reactive astrogliosis in a hallmark of HAND and is also associated with an increase in secreted inflammatory markers, we also analyzed the levels of glial fibrillary acidic protein (GFAP), an astrocyte protein that elevated during astrogliosis. The data in **Fig. 3A** shows a decreased expression in CCF-STTG1 (8% reduction, lane 1 *vs*. 2) and U138 cells (29% reduction, lane 3 *vs*. 4). These findings suggest that the EV-mediated changes in secreted inflammatory proteins are not due to state of reactive astrogliosis. Given these findings, cell proliferation was assessed to confirm cell cycle inhibition and a senescent state. The results in **Fig. 3B** show that cellular ATP was significantly decreased in cells treated with EVs from untreated, HIV-1 infected donor MDMs (lanes 2 and 5; $p< 0.001$). Similarly, cART treated, HIV-1 infected donor MDM EVs (lanes 3 and 6) also elicited a reduction in cellular ATP in recipient cells ($p<0.001$ and $p<0.01$, respectively) albeit to a lesser extent, which suggests that cART can potentially alter EV cargo loading, as we have shown previously[36]. Although CellTiter-Glo assay is typically used as an indicator of cell viability, microscopy of EV-treated cells showed no change in morphology of the treated astrocytes (**Fig. 3C**). Therefore, these results suggest an EV-mediated non-proliferative state.

EVs secreted from HIV-1 infected MDMs elicit production of proinflammatory cytokines in astrocytes

Since a decrease in intracellular inflammatory proteins was seen in astrocytes upon EV treatment, we hypothesized that the data would correlate with an increased extracellular secretion of inflammatory proteins. To investigate this, astrocytes were either treated with EVs isolated from MDMs treated with cART or a senescence drug inducer, sodium butyrate, and incubated for two timepoints (24 and 72 hours) to examine protein expression over time. Supernatants were collected and EVs were Western blotted for IL-6 and MMP3. The data in **Fig. 4A** demonstrates very high EV-mediated IL-6 secretion in CCF-STTG1 astrocytes with an 72% increase compared to the untreated control (lane 2 vs 1). Overtime, EV-mediated IL-6 secretion increased by 40%, while the sodium butyrate-mediated IL-6 secretion increased by 137% (lanes 2 and 5; 3 and 6). Similarly, U138 astrocytes showed an 13% (24 hour) and 20% (72 hour) increase in IL-6 secretion upon EV treatment compared to the untreated control, although it (**Fig 4B**; lanes 1 and 2; 4 and 5). Both cell lines showed varied extracellular levels of MMP3 expression with EV treatment compared to untreated lanes (**Fig. 4A-B**; lanes 1 and 2). Taken together, these findings imply that there indeed is secretion of proinflammatory cytokines, IL-6 and MMP3, from astrocytes induced by EVs released from HIV-1 MDMs, despite antiretroviral treatment.

TAR inhibitors lower EV-mediated TLR3 activation and downstream proinflammatory cytokine production

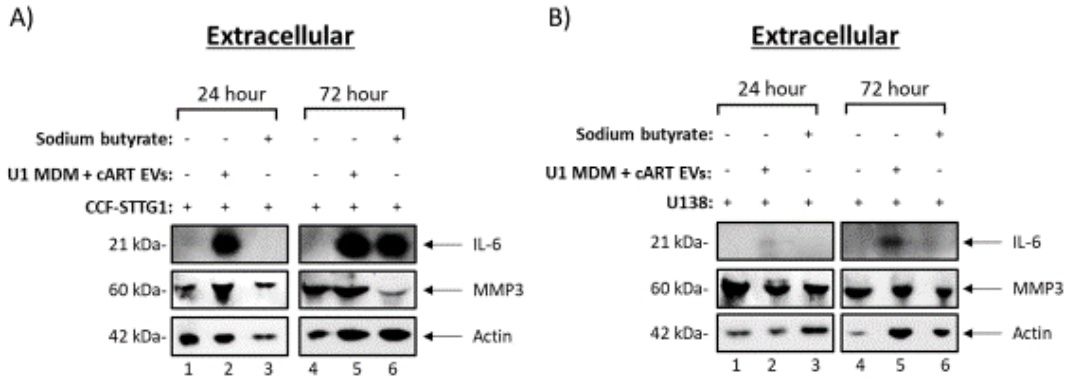

Figure 4. EVs from HIV-1 infected MDMs induce secretion of proinflammatory cytokines from Astrocytes. U1 cells were cultured for 5 days. U1 monocytes were differentiated into MDMs using PMA (100 µM) and treated with ± cART cocktail (10 µM; Darunavir, Emtricitabine, Tenofovir, and 5 µM Ritonavir) for 5 days. **A**) CCF-STTG1 and (**B**) U138 cells (1 x 10^6 each) plated and treated with EVs released from MDMs treated with cART (1:10,000 cell to EV ratio) and Sodium butyrate (1 mM). Supernatants were collected at 24 and 72 hours and enriched for EVs using NT80/82 beads, followed by SDS-PAGE and Western Blot analysis for pro-inflammatory markers (IL-6 and MMP3) and Actin.

Our previous studies have found that EVs released from HIV-1 infected cells contain TAR RNA, a 59-nucleotide, small, non-coding RNA that is produced in infected cells as a result of non-processive transcription[10,36,57]. The presence of TAR RNA within EVs has been confirmed in patient biofluids, including CSF, despite suppressive antiretroviral therapy[36]. Additional studies by our lab showed that EV-encapsulated TAR RNA can bind Toll-like Receptor 3 (TLR3), a receptor of the innate immune system involved in the sensing of double-stranded RNA, in recipient myeloid cells to elicit an increase in the production of proinflammatory cytokines through activation of the NF-κB pathway[10]. TLR3 is expressed in numerous cell types including several within the CNS such as glia (microglia, astrocytes and oligodendrocytes) and neurons, therefore, we questioned whether EV-mediated TLR3 activation could play a role in chronic neuroinflammation observed in long-term, cART-treated patients[58–60]. To ensure the relevance of this question, we first examined several cell types involved in HIV-1 pathogenesis. Cell lysates from T-cells (CEM and Jurkat), uninfected and infected monocytes (U937 and U1), astrocytes (CCF-STTG1), and neurons were analyzed via Western blot for the presence of TLR3. The data in **Fig. 5A** shows the presence of TLR3 in all cell types investigated, which suggests that EV-mediated TLR3 activation could potentially occur in the aforementioned cell types.

In order to confirm TLR3 activation by TAR RNA, we utilized an *in vitro* kinase assay. The results in **Fig. 5B** show a dose-dependent increase in TLR3 phosphorylation upon the addition of TAR RNA, validating our previous findings. These results were quantitated using densitometry analysis (**Fig. 5C**) which showed an 83-94% increase in

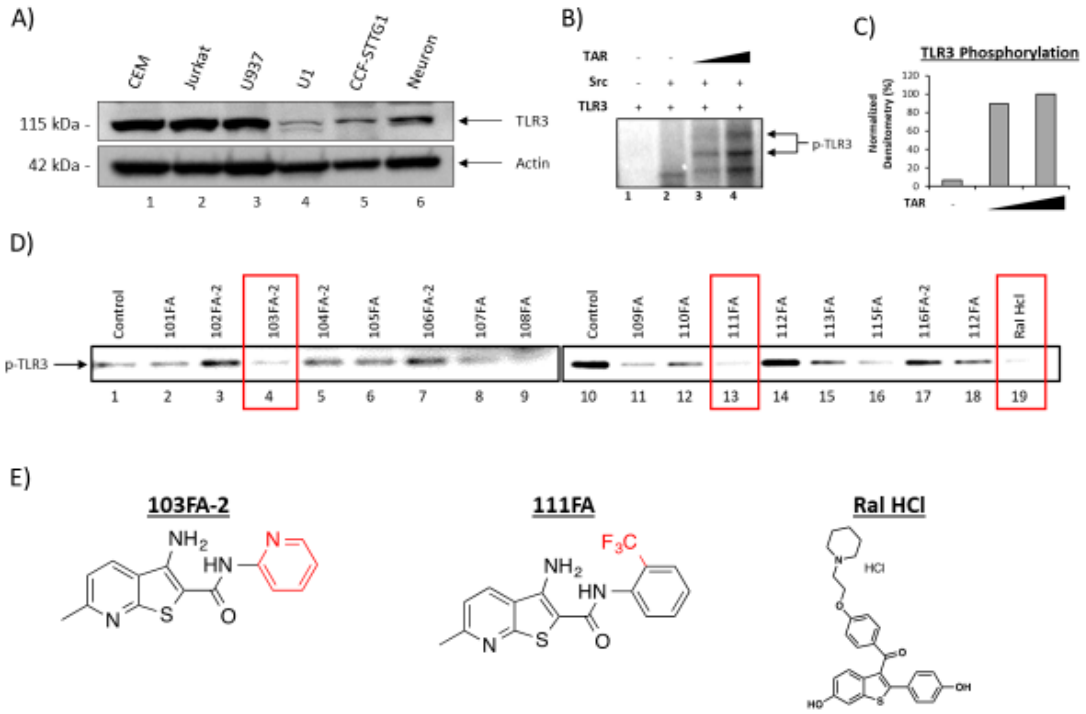

Figure 5. HIV-1 TAR RNA inhibitors block TLR3 activation. **A**) Uninfected T-cells (CEM and Jurkat), uninfected monocytes (U937), infected monocytes (U1), astrocytes (CCF-STTG1) and neurons were lysed and analyzed via Western blot to confirm the presence of TLR3 with Actin as a control. **B**) Confirmation of TLR3 activation by src kinase in presence of double stranded TAR RNA was assessed using an in vitro kinase assay which utilized purified TLR3 protein (100 ng), purified Src kinase (10 ng), and TAR RNA (10 and 100 ng) and run through SDS-PAGE. The blot was then imaged with phosphor-imager. **C**) Densitometry analysis of in vitro kinase assay was performed using ImageJ software to obtain raw densitometry counts relative to background. The counts are shown as relative expression of the protein relative to highest phosphorylation levels (lane 3; set to 100%). **D**) Follows a similar experimental design as panel C coupled with a panel of TAR inhibitors (1 µM). **E**) Chemical structures of TAR inhibitor compounds.

phosphorylation of TLR3 in the presence of TAR RNA. To inhibit this phosphorylation and subsequent activation, we utilized a panel of 17 small molecules which have previously been found to bind HIV-1 TAR RNA[61], and screened them for their ability to inhibit TLR3 activation using an *in vitro* kinase assay. The results in **Fig. 5D** identified three potential candidates, 103FA-2, 111FA, and Ral HCl, that were effective in reducing the phosphorylation of TLR3.

As activation of the TLR3 pathway can result in downstream production of proinflammatory cytokines, such as IL-6, we hypothesized based on our previous findings that the TAR inhibitors can also lower downstream production of proinflammatory cytokines. To confirm this, CCF-STTG1 astrocytes were treated with EVs from U1 MDMs treated with cART, as well as a titration of the same TAR inhibitors that lowered TLR3 activation (103FA-2, 111FA, Ral-HCl; 100, 10, 1 nM) for 3 days. EVs from the supernatants were enriched using NT80/82 beads and Western blotted for IL-6. The data in **Fig. 6** shows that drastic increase in production of IL-6 from the U1 MDM treated with cART EV, compared to the untreated control and U937 EV treatment (98% and 85%; lane 3 vs 1 and 2). Additionally, all three TAR inhibitor compounds showed similar trends of a decrease in IL-6 production as concentration increases (maximum 51% reduction), indicating that there is lowered IL-6 production with TAR inhibitor treatment.

Cannabidiol inhibits the release of EVs from HIV-1 infected monocytes

We and other colleagues have previously shown that EVs released from virally infected cells contain viral products which can contribute to viral pathogenesis, specifically

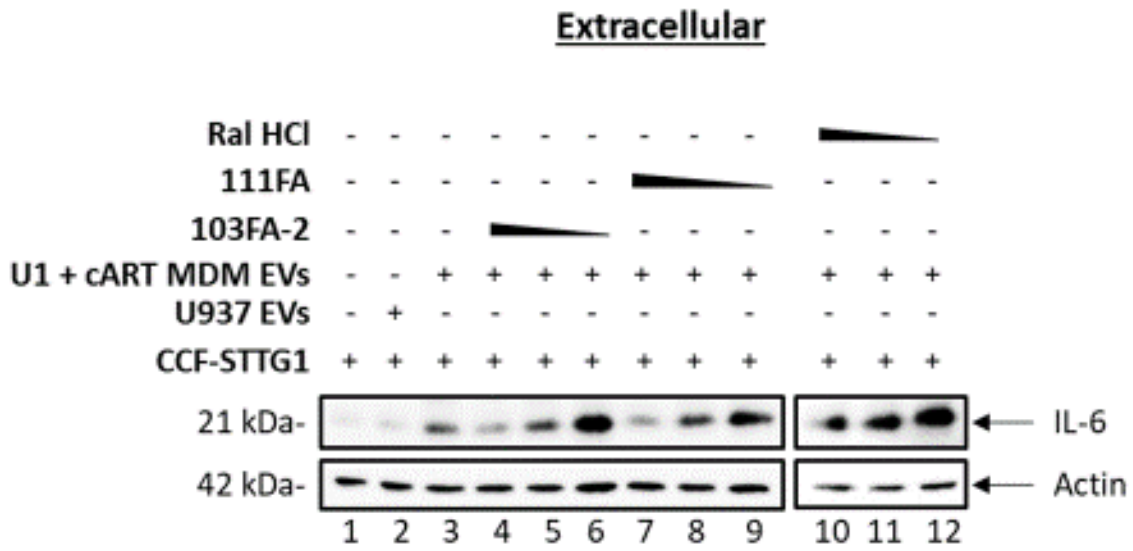

Figure 6. HIV-1 TAR inhibitors lower proinflammatory cytokine production in astrocytes. U937 and U1 cells were cultured for 5 days. U1 monocytes were differentiated into MDMs using PMA (100 µM) and treated with ± cART cocktail (10 µM; Darunavir, Emtricitabine, Tenofovir, and 5 µM Ritonavir) for 5 days. EVs were isolated using ultracentrifugation and assessed for concentration and particle size using ZetaView to equilibrate EV concentrations. EVs were used to treat astrocytes (CCF-STTG1; 1 x 10^6) at a 1:10,000 concentration (cell/EVs ratio). CCF-STTG1 cells were treated with ± EVs from U937 cells, as well as U1MDMs that were treated with cART (10 µM; Darunavir, Emtricitabine, Tenofovir, and 5 µM Ritonavir) at a 1:10,000 concentration (cell/EVs ratio), and ± titration of TAR inhibitors (1, 10, and 100 nM; 103FA-2, 111FA, and Ral HCL) for 3 days. Supernatants from the cells were nanotrapped and western blotted for pro-inflammatory markers: IL-6 and Actin.

inflammation in those with long-term, chronic infections such as HIV-1[10,12]. Furthermore, we have shown that EVs released from infected cells contain viral proteins and RNAs despite treatment with HIV-1 specific antiretrovirals as well as general antivirals such as interferon-α[12], suggesting a potential gap in standard of care treatments. Therefore, we reasoned that CBD, which has previously been found to have significant anti-inflammatory properties[62], could mitigate the enhanced inflammation observed in long-term HIV-1 patients through modulation of EV release from infected cells. To this end, HIV-1 infected monocytes (U1) were treated twice with a titration of CBD (1, 5, and 10 μM) over 5 days with no reduction in cell viability (data not shown). Supernatants were harvested and analyzed using ZetaView NTA. The data in **Fig. 7A** suggests that treatment with CBD results in a significant reduction in the number of EVs released from virally infected cells, specifically, treatment with CBD (1, 5, and 10 μM; lanes 2-4) resulted in a 44, 76, and 79% decrease in EVs, respectively, as compared to an untreated control.

To verify that the observed decrease in EVs was not the result of modifications in packaging of various cargos into larger EVs, the mean diameter size (**Fig. 7B**), median diameter size (**Fig. 7C**), and peak diameter size (**Fig. 7D**) were also analyzed. Treatment with either concentration of cannabinoid (1, 5, and 10 μM or μg/mL, respectively) resulted in little to no change in diameter.

Cannabidiol decreases EV-associated viral proteins

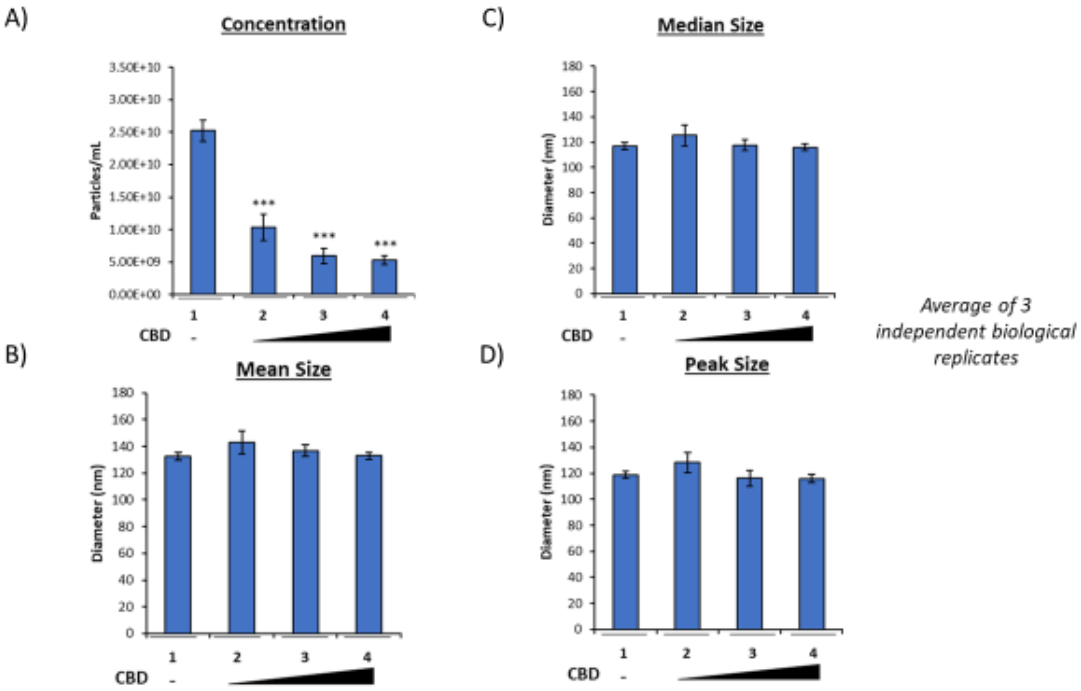

Figure 7. CBD lowers EVs released from HIV-1 infected monocytes. HIV-1 infected U1 monocytic cells (1 x 10^6) were treated with a titration of CBD (1, 5, and 10 uM) every day for 5 days (Temple). Cells were pelleted and supernatant was used for Zetaview NTA analysis to determine (**A**) EV concentration, (**B**) median size, (**C**) mean size, and (**D**) peak size. Each bar represents an average of three independent replicates. Student T-test was used for statistical analysis comparing treated (lanes 2-4) with untreated control (lane 1), where * p-value ≤ 0.05; ** p-value ≤ 0.01, *** p-value ≤ 0.001.

We have previously shown that, despite cART, EVs released from HIV-1 infected cells contain viral protein and RNA which can elicit detrimental effects in uninfected recipient cells[63–66]. To verify that cannabinoid treatment not only results in a reduction in EV number, but also a reduction in the presence of viral products, cells were treated twice with a titration of CBD and incubated for 5 days. Following incubation, supernatants were collected and EVs were enriched using NT80/82 particles, which have previously been shown to be effective in enriching EVs from low volume culture supernatants[1,9,10,66–68]. Enriched samples were then analyzed by Western blot for the presence of EV marker proteins and HIV-1 viral proteins. The data in **Fig. 8A** confirm the findings in **Fig. 7A**, as the levels of CD81, a tetraspannin protein associated with EVs, specifically exosomes, were decreased upon addition of CBD (1, 5, and 10 μM; lanes 2-4). The most drastic decrease in CD81 expression was achieved by low titer CBD, which resulted in an 80% reduction as indicated by densitometry analysis (data not shown).

The viral protein, Nef, has previously been found to be incorporated into EVs by numerous cell types, including those of the CNS such as astrocytes and microglia. Further evidence has identified Nef as a potential contributor to HIV-1 pathogenesis through various mechanisms including the promotion of secreted proinflammatory cytokines, the suppression of neuronal action potentials, and disruption of the blood-brain barrier (BBB)[66,69–72]. Data in **Fig. 8A** illustrates a dose-dependent decrease in EV-associated Nef (30 kDa) and its membrane-associated myristoylated Nef dimer (70 kDa) upon treatment

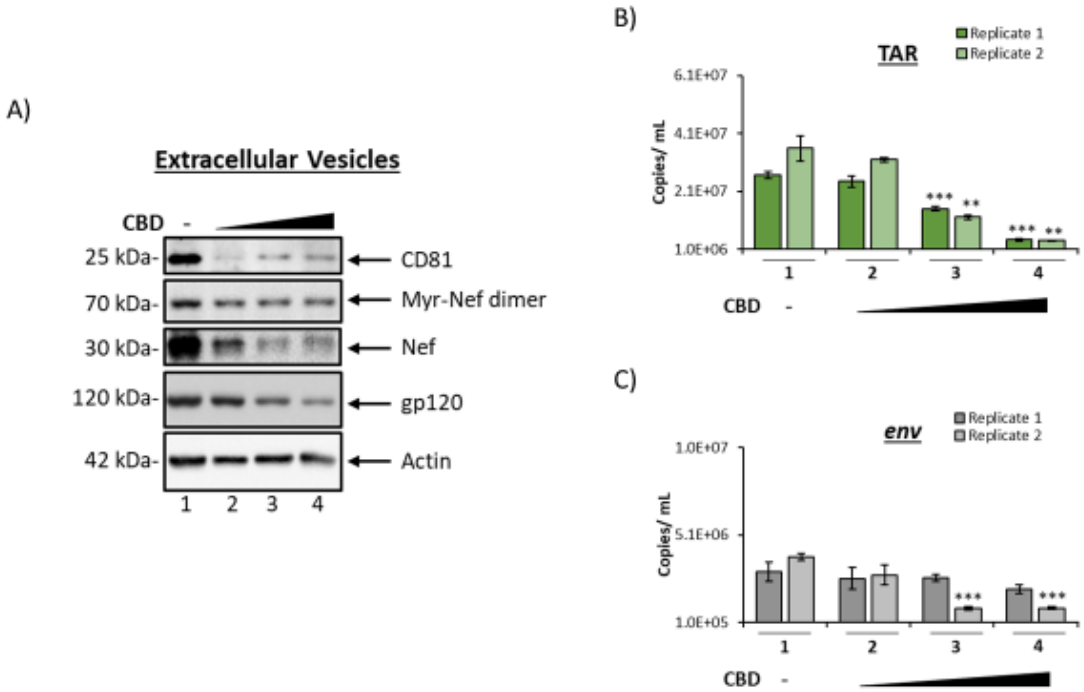

Figure 8. CBD decreases secretion of viral proteins and RNA from HIV-1 infected monocytes. U1 cells (1 x 10^6) were treated with a titration of CBD (1, 5, 10 uM) every day for 5 days (Temple). Cellular supernatant was collected, exosomes were enriched with nanoparticles (NT80/82) beads overnight at 4°C, (**A**) pelleted, run through SDS-PAGE, and western blotted for exosomal (CD81) and HIV-1 viral markers (myr-Nef, Nef, gp160, gp120), as well as actin. **B**) Following the same experimental design as (A), cellular supernatant was nanotrapped and pelleted. RNA was isolated from the samples, followed by RT-qPCR analysis for HIV-1 viral transcripts, TAR and (**C**) env. Student T-test was used for statistical analysis comparing treated (lanes 2-4) with untreated control (lane 1), where * p-value ≤ 0.05; ** p-value ≤ 0.01, *** p-value ≤ 0.001.

with CBD. Densitometry analysis (data not shown) suggests there is a more drastic decrease in the lower molecular weight form of Nef (up to 79%, lane 3) as compared to the myristoylated dimer (up to 37%, lane 7).

Gp120 can contribute to enhanced HIV-1 infection of the CNS and the corresponding neuroinflammation through disruption of the BBB, increased cytokine secretion, specifically Tumour Necrosis Factor alpha (TNFα), a proinflammatory cytokine, via activation of microglia and astrocytes, and increased neuronal sensitivity to calcium fluctuation[73–80]. Numerous studies have shown the potential of endogenous cannabinoids, or endocannabinoids, to alleviate gp120-induced neuroinflammation in HIV-1 infection (Reviewed in [81]). Therefore, we reasoned that CBD, which target the same receptors as endocannabinoids, could also result in a reduction in EV-associated gp120. Results in **Fig. 8A** show a reduction in EV-associated gp120 ranging from 39-58% with CBD treatment, suggesting a potential to mitigate the gp120-induced neuropathogenesis. Interestingly, the titration of both cannabinoids elicited an increase in the presence of gp160, the HIV-1 precursor glycoprotein. However, CBD induced an increase in gp160 by up to 125% (lane 4), as measured by densitometry (data not shown). This is in line with a corresponding decrease in the presence of the processed envelope glycoprotein, gp120, suggesting that both cannabinoids could potentially interfere with the proteolytic cleavage of HIV-1 precursor polyproteins, potentially through modulation of intracellular Ca^{2+} levels as the primary endoprotease responsible for cleavage is a calcium-dependent enzyme[82]. Therefore, CBD may also contribute to the levels of EVs containing unprocessed glycoprotein or also defective viral particles.

Similar to viral proteins, HIV-1 infections lead to the incorporation of viral RNAs into EVs released from infected cells. HIV-1 TAR RNA is a short, non-coding RNA produced in infected cells as a result of non-processive transcription. We and other colleagues have found TAR RNA to be incorporated into EVs released from infected cells and can be detected in several biofluids at high copy numbers[10,12,57]. TAR within EVs has been shown to expand viral pathogenesis through down-regulation of apoptosis, increased susceptibly to HIV-1 infection, and activation of TLR3 to subsequently stimulate the production of pro-inflammatory cytokines within uninfected recipient cells[10,57]. To determine if cannabinoids possessed the potential to limit the incorporation of such RNAs into EVs, the same supernatants were enriched for EVs using NT80/82 particles, total RNA was isolated and subjected to RT-qPCR for the presence of TAR RNA, a short non-coding HIV-1 RNA, and viral full-length genomic RNA, *env*. The results in **Fig. 8B** show a dose-dependent decrease in the presence of EV-associated TAR RNA following addition of CBD (lanes 2-4). All doses of CBD elicited a reduction in TAR RNA as compared to the control (lane 1). A statistically significant decrease in TAR RNA within EVs was observed in the two highest concentrations (5 and 10 μM), which produced an average of 55%, and 86% reduction, respectively, from two replicates. Similarly, treatment with CBD resulted in the reduction of *env* RNA within EVs (**Fig. 8C**). Taken together, these results indicate that CBD decreases the number of EVs released from HIV-1 infected cells, which leads to a decrease in the amount of viral products (protein and RNA) available to contribute to chronic inflammation.

Although the effects of CBD seem optimal at a cell line *in vitro* model, it is important to analyze and determine whether similar results could be obtained in human cells, such as primary macrophages, for clinical relevancy. To examine whether the same trend could be observed in a primary cell model, three independent replicates of HIV-1 infected primary macrophage cells were treated with a titration of CBD (1, 5, and 10 μM). EVs were enriched from the extracellular supernatant using NT80/82 beads and analyzed for HIV-1 TAR and *env* (**Fig 9**). Data in **Figure 9A** demonstrates a correlation between increased CBD treatment and statistically significant decrease in TAR RNA within EVs from all three infected primary macrophages. Additionally, a similar statistically significant decreasing trend is observed with the amount of *env* RNA in secreted EVs released from two out of three infected primary macrophages (**Fig. 9B**).

Cannabinoids inhibit HIV-1 transcription in monocytes

Given that our results indicate a reduction in EV release and EV-associated HIV-1 viral RNAs and proteins, we hypothesized that the observed reduction could be the result of changes in viral transcription resulting a decreased production of viral products available for release from the cell in EVs. Therefore, U1 monocytes were treated with a titration of CBD (1, 5, 10 μM) every day for 5 days. RNA was isolated from the harvested cell pellets, followed by RT-qPCR analysis of 3 independent replicates for TAR and *env* RNAs. Both TAR and *env* viral RNAs exhibited a dose-dependent decrease in response to CBD treatment (**Figure 10A**; lanes 2-4 vs lane 1), with the highest dose (lane 4; 10 μM) resulting

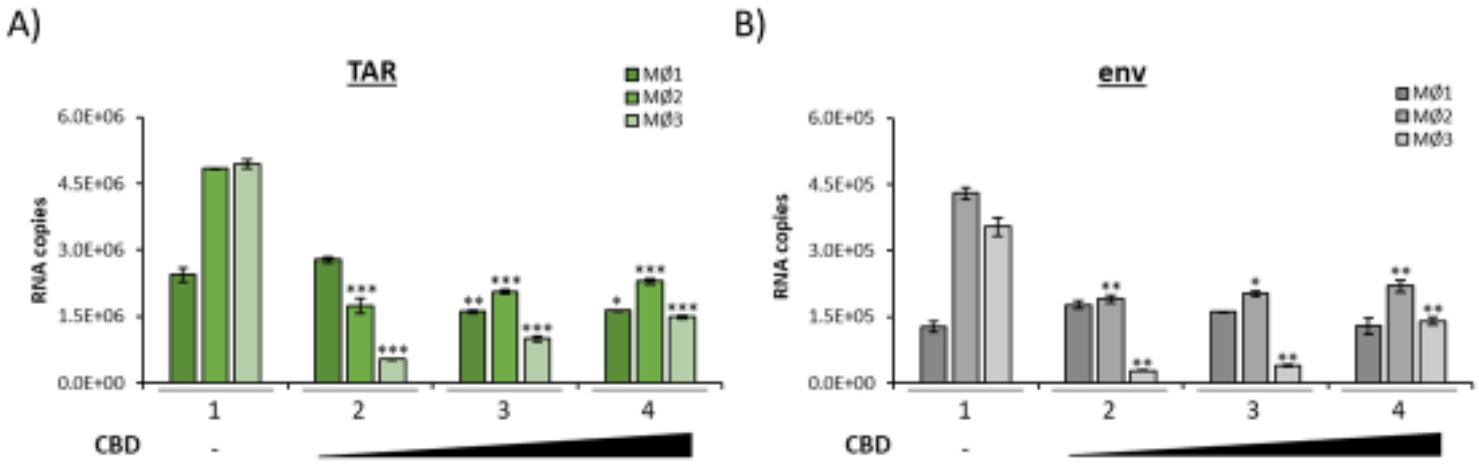

Figure 9. CBD lowers viral RNA secreted from HIV-1 infected primary macrophages. HIV-1 infected primary macrophages (1 x 10^6) were treated with a titration of CBD (1, 5, 10 uM) every day for 5 days. Supernatant was then isolated and exosomes were enriched using NT80/82 beads overnight at 4 °C. The NT80/82 beads were then pelleted, RNA was isolated, followed by RT-qPCR analysis for **A**) TAR and (**B**) env viral RNA transcripts. These are an average of 3 replicates. Student T-test was used for statistical analysis comparing treated (lanes 2-4) with untreated control (lane 1), where * p-value ≤ 0.05; ** p-value ≤ 0.01, *** p-value ≤ 0.001.

in a 95% and 96% decrease as compared to the untreated control. This potentially indicates that the reduction in secreted EV-associated viral TAR and *env* RNAs may be the result of CBD-mediated transcription inhibition. Furthermore, the reduction in both TAR and full length genomic (*env*) RNA suggest that CBD has the potential to inhibit viral transcription at the level of transcription initiation.

To verify that the CBD-mediated transcription inhibition resulted in a decrease in the production of viral proteins within HIV-1 infected cells, U1 cells were treated with a titration of CBD (1, 5, 10 μM) every day for 5 days and intracellular lysate was used for Western blot analysis of specific viral proteins, Nef, Pr55, and p24. As expected, intracellular levels of Nef, Pr55, and p24 proteins were downregulated post-CBD treatment in a dose dependent manner (**Figure 10B**). The most significant reduction in all three viral proteins Pr55 (99%), p24 (76%), and Nef (62%) was observed with the 10 μM concentration of CBD (densitometry data not shown). This is potentially due innate differences in the abundance of these mRNAs. Overall, there are typically fewer *gag* (Pr55/p24) mRNA transcripts within HIV-1 infected cells as compare to compared to *nef* mRNAs, which account for nearly 50% of all HIV-1 doubly spliced RNA in infected cells[83].

Cannabinoids lower EV-mediated inflammation from astrocytes

Previously we have shown that EVs released from HIV-1 infected MDMs cause astrocyte- mediated inflammation through TLR3 activation, which mechanism and subsequent effects can be lowered using TAR inhibitors (**Fig. 4-6**). To examine the

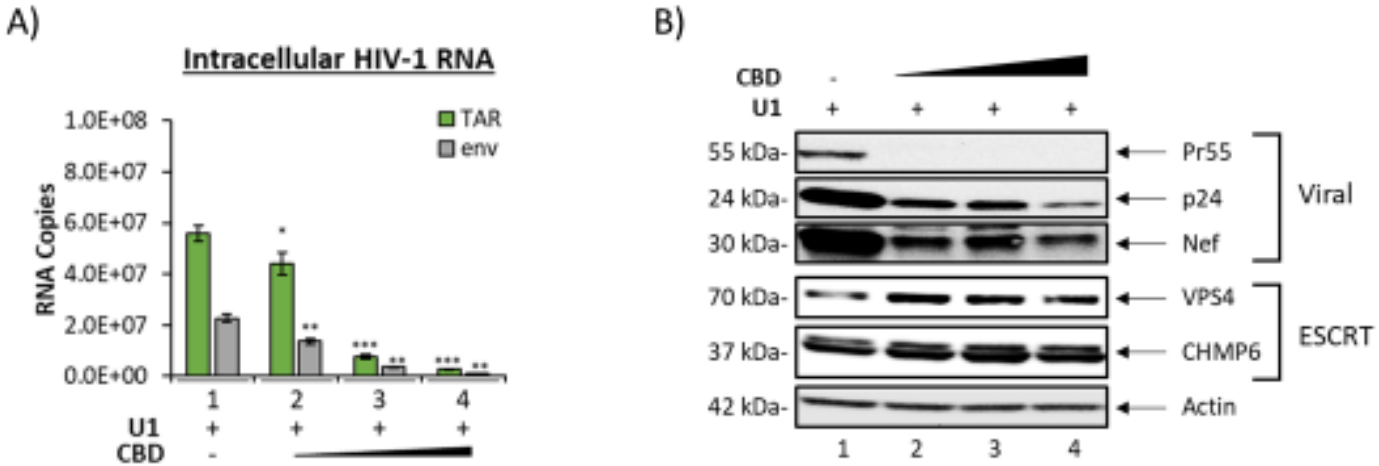

Figure 10. CBD lowers intracellular viral RNA and proteins in HIV-1 infected monocytes. U1 cells (1 x 10^6) were treated with a titration of CBD (1, 5, 10 uM) every day for 5 days (Temple). **A**) Intracellular RNA was isolated and analyzed through RT-qPCR for HIV-1 viral transcripts TAR and env. Each bar represents an average of three independent biological replicates. **B**) Cells pellets were lysed, run through SDS-PAGE, and western blotted for EV biogenesis marker VPS4, viral markers (gp120, Nef, pr55, and p24), and Actin. Student T-test was used for statistical analysis comparing treated (lanes 2-4) with untreated control (lane 1), where * p-value ≤ 0.05; ** p-value ≤ 0.01, *** p-value ≤ 0.001.

anti-inflammatory effects of CBD, in terms of HIV-1 infection, on EV-mediated CNS inflammation, CCF-STTG1 astrocytes were treated with a titration of CBD (1, 5 10 μM) and U1 MDM EVs (1:10,000 ratio; cell/EV) for 3 days. EVs from supernatants were enriched using NT80/82 particle beads and Western blotted for expression of extracellular IL-6. The data in **Fig. 11** demonstrates that IL-6 secretion was decreased with increasing concentrations of CBD with the maximum reduction at 123% and 211% (lane 3 vs lane 5 and 6; normalized densitometry not shown), similar to the trend seen with TAR inhibitor treatment (in **Fig. 6**). This suggests that CBD can be used to reduce EV-mediated inflammation produced by astrocytes.

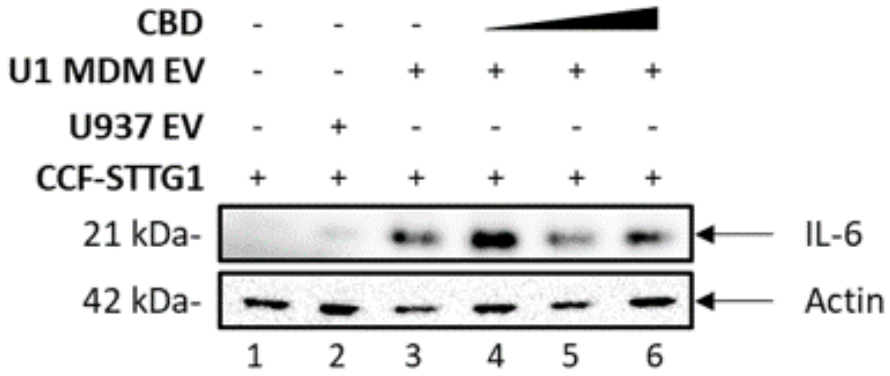

Figure 11. CBD reduces proinflammatory effects induced by EVs released from HIV-1 infected MDMs. EVs from U937 and U1 MDMs were treated onto CCF-STTG1 astrocytes (5 x 10^5) at a 1:10,000 (cell/EV) ratio for 3 days. Supernatants were isolated and EVs were enriched using NT80/82 beads, followed by SDS-PAGE and Western blotted for Il-6 and Actin.

DISCUSSION

We and others have previously shown that, despite effective viral suppression by cART, viral reservoirs, including the CNS, are transcriptionally active, resulting in the production of short, non-coding and full length genomic RNAs via non-processive and basal transcription, respectively. This is evident by a number of studies which report the persistence of approximately $1x10^3$ copies of cell-associated RNA in both circulating $CD4^+$ T-cells [7,84] and myeloid cells from several brain regions[8]. Furthermore, we have found that these RNAs and their respective proteins can be packaged into EVs and released from the cell to elicit changes in uninfected recipient cells[10,36,57]. In line with this, we have shown here that cART, specifically those drugs that are utilized in the treatment of individuals with CNS infection, caused an increase in the secretion of larger vesicles from monocytes (**Fig. 1**), which may suggest the alteration of other mechanisms such as the autophagy pathway and, in turn, increased secretion of autophagosomes. Autophagy, specifically mitophagy (a form of selective mitochondrial autophagy), is essential for basal turnover in cells and is of particular importance in maintaining neuronal homeostasis. Disruption of autophagy and/or mitophagy has been implicated in many chronic neurodegenerative diseases, such as Alzheimer's disease, Parkinson's disease, Multiple Sclerosis, Amyotrophic Lateral Sclerosis, and transmissible spongiform encephalopathies (i.e. prion diseases)[85–87], suggesting the potential for elevated EV release. Along these lines, EVs have

been shown to contribute to propagation of these diseases via the transfer of various cargos, including misfolded proteins, from diseased cells to healthy cells[88–97]. It follows that the induction of autophagy through inducers, such as those used in this study, could be explored as potential therapeutics to prevent or slow the progression of neurodegenerative diseases beyond HIV-1 neurological pathologies. Given the pivotal role of basal autophagy, including selective autophagy, in cellular homeostasis and quality control, it is not surprising that excessive reduction in these processes can elicit and contribute to disease. It follows that viruses, including HIV-1, have evolved ways to either circumvent degradation of viral proteins through these processes, and that drugs used in the treatment of infection could potentially exacerbate these effects. Considering the many forms of autophagy and the diverse changes in these processes regarding disease, further research is needed to develop more specific modulators of autophagy to allow for precise targeting of the disease mechanism.

Previous studies from our lab have shown that EVs containing TAR RNA can promote HIV-1 pathogenesis in recipient uninfected cells by eliciting an increase in proinflammatory cytokines and susceptibility to infection in recipient circulating immune cells[10,36,57]. Here, we show for the first time that EVs from HIV-1 infected myeloid cells can elicit change in recipient astrocytes in terms of alteration in cell cycle progression and increased production of pro-inflammatory proteins (**Fig. 3-4**), which could have broad implications for HIV-1 patients including a reduction in the maintenance and support of neurons. More specifically, our findings suggest that EVs potentially can induce the inflammatory response mechanism of astrocyte senescence and the associated secretory

phenotype through TLR3-mediated activation (**Fig. 3-5**). The secretory phenotype elicited by EV-treatment can multiply the inflammatory state of the CNS. For example, HMGB1 has been found to be involved in several neurodegenerative diseases including demyelinating diseases like multiple sclerosis[98,99], non-demyelinating neurological diseases such as Amyotrophic Lateral Sclerosis[100], and epilepsy[101]. Furthermore, HMGB1 can contribute to BBB dysfunction[102] and therefore may exacerbate BBB leakiness in HIV-1 infection.

The high abundance of HIV-1 TAR RNA in patient biofluids and tissues as well as the presence of TAR RNA in the majority of tested patient materials suggests that the impacts of TAR RNA could potentially have far-reaching effects. Our data confirms our previous studies by our lab which demonstrate that EV-associated HIV-1 TAR RNA can activate TLR3 in recipient cells thereby contributing to chronic immune activation (**Fig. 5A-B**). In general, the TLR3 signaling cascade can stimulate the transcription of Type I Interferons via IRF3 and can activate the NF-κB pathway to produce pro-inflammatory cytokines. The data presented here suggests that activation of TLR3 by EVs from infected myeloids may activate the IRF3 signaling cascade to promote cell cycle arrest and senescence in astrocytes (**Fig. 5**). However, EV-mediated activation could also activate the NF-κB pathway. NF-κB transcription factors are abundant within the CNS and can play both a protective and toxic role depending on the type of signaling[103]. While constitutive NF-κB signaling can provide neuroprotection, induction of NF-κB through various stimuli, such as TLR3 activation, has been found to contribute to neurological damage through several mechanisms. Induced NF-κB signaling can exert its effects on endothelial,

neuronal, and glial cells. This induction leads to vascular inflammation and increased permeability of the BBB, neuronal cell death, as well as neurodegeneration and inflammation in glial cells, all of which are hallmarks of HAND. Furthermore, NF-κB has been implicated in the induction of senescent phenotypes in a number of different models and senescent astrocytes have been associated with chronic neurocognitive disorders such as Alzheimer's disease[108–110]. Overall, astrocytes play a vital role in the support and maintenance of heathy neurons and play a pivotal role in the progression of CNS dysfunction in chronic diseases. Therefore, this potential EV-mediated TLR3 activation mechanism requires further investigation, specifically in the context of other CNS cell types or brain models.

To combat this EV-mediated mechanism, we have screened a panel of small molecule TAR RNA binding compounds for their ability to bind TAR RNA and inhibit activation of TLR3 in recipient cells. Our findings show three compounds, 103FA-2, 111FA, and Ral HCl could be utilized to selectively inhibit TLR3 activation by TAR RNA while maintaining innate immune function due to targeting of the ligand rather than the receptor (**Fig. 5B-C**). Furthermore, findings involving small TAR-binding molecules suggest that the changes in astrocyte are likely due to the activation of TLR3 by EV-associated TAR RNA (**Fig. 5D**). TLR3 is abundant in multiple CNS cell types and some evidence suggests that TLR3 is localized to the cell surface in astrocytes, potentially making them more vulnerable to TAR RNA-containing EVs[58]. However, EVs possess a wide array of RNA cargo including numerous cellular RNAs and, as such, the possibility of cellular RNA contributions to TLR3 activation cannot be ruled out. In line with this,

TLR3 expression has been found to be enhanced in the brains and spinal cords of individuals with chronic neuroinflammation, such as those with Multiple Sclerosis or Alzheimer's disease[58,111,112], suggesting these findings could potentially be applied to cellular RNAs encapsulated in EVs and their contributions to other chronic neurocognitive disorders.

In addition, CBD has been FDA-approved for preventative treatment of epileptic seizures and has also shown promising implications in lowering inflammation in several cancer diseases, as aforementioned above. From this, we rationalized and demonstrated that, in the context of HIV-1, CBD could be used as a potential treatment option for countering inflammation by lowering the release of proinflammatory EVs released from HIV-1 infected monocytes, as well as their viral contents (**Fig. 7-9**). We briefly identified a potential mechanism by which CBD may cause the over lowering of secretion of EVs and production of viral non-coding and genomic RNAs, which is through lowering viral transcription (**Fig. 10A**). The decreased transcription of TAR and *env* RNAs may lead to lowered viral products being transcribed (**Fig. 10B**). Additionally, the lack of decrease in exosomal biogenesis, or ESCRT, markers from CBD treatment, despite decrease in EV release, requires more investigation as to the mechanism that CBD may potentially use to lower EV release, such as looking at other EV biogenesis markers such as microvesicle biogenesis or autophagy pathways. Although CBD lowers the transcription of intracellular viral RNAs, there are still high RNA copies with treatment, which may suggest that CBD may lower transcription indirectly through mechanisms such as polymerase II activity inhibition or inducing chromosome closed formation by preventing phosphorylation of

histone, H1, which would inhibit transcription of viral RNAs. Furthermore, the direct inhibition of IL-6 production from proinflammatory EV treatment in astrocytes by CBD directly highlights the anti-inflammatory prospects of CBD in a viral *in vitro* model, as well as an *in vitro* CNS model (**Fig. 11)**. Overall, we determined that CBD and TAR inhibitors shows promise in lowering inflammation seen in HAND, while antiretroviral therapy contributes to the inflammation in HAND (**Fig. 12**). Although astrocytes consist of the predominant part of the CNS, it would be interesting to inquire as to whether CBD can lower inflammation in other CNS cells such as microglia and neurons, as well as in HAND patients. Since CBD has already been approved for treatment of epilepsy, it could potentially be repurposed for HAND patients based on our promising results.

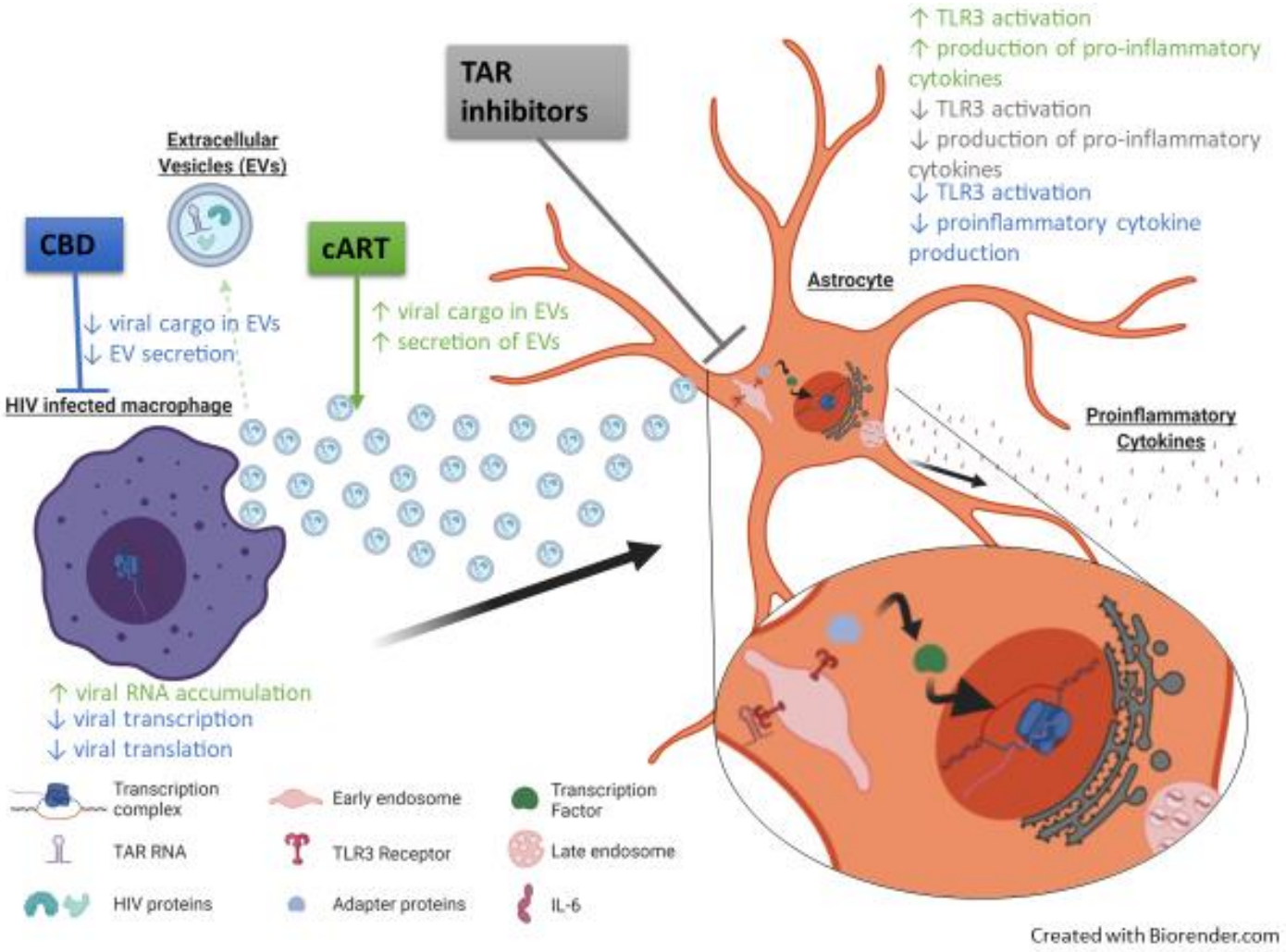

Figure 12. Summary of effects of proinflammatory EVs released from HIV-1 infected myeloids on astrocytes.

REFERENCES

1. Barclay, R. A. *et al.* Exosomes from uninfected cells activate transcription of latent HIV-1. *J. Biol. Chem.* **292**, 11682–11701 (2017).
2. Akpamagbo, Y. A. *et al.* HIV-1 Transcription Inhibitors Increase the Synthesis of Viral Non-Coding RNA that Contribute to Latency. *Curr. Pharm. Des.* (2017) doi:10.2174/1381612823666170622101319.
3. Global HIV & AIDS statistics — 2019 fact sheet. https://www.unaids.org/en/resources/fact-sheet.
4. Basic Statistics | HIV Basics | HIV/AIDS | CDC. https://www.cdc.gov/hiv/basics/statistics.html (2020).
5. Arts, E. J. & Hazuda, D. J. HIV-1 Antiretroviral Drug Therapy. *Cold Spring Harb. Perspect. Med.* **2**, (2012).
6. Saylor, D. *et al.* HIV-associated neurocognitive disorder — pathogenesis and prospects for treatment. *Nat. Rev. Neurol.* **12**, 234–248 (2016).
7. Hatano, H. *et al.* Cell-Based Measures of Viral Persistence Are Associated With Immune Activation and Programmed Cell Death Protein 1 (PD-1)–Expressing CD4+ T cells. *J. Infect. Dis.* **208**, 50–56 (2013).
8. Kumar, A. M., Borodowsky, I., Fernandez, B., Gonzalez, L. & Kumar, M. Human immunodeficiency virus type 1 RNA Levels in different regions of human brain:

Quantification using real-time reverse transcriptase-polymerase chain reaction. *J. Neurovirol.* **13**, 210–224 (2007).

9. Jaworski, E. *et al.* The use of Nanotrap particles technology in capturing HIV-1 virions and viral proteins from infected cells. *PloS One* **9**, e96778 (2014).
10. Sampey, G. C. *et al.* Exosomes from HIV-1-infected Cells Stimulate Production of Pro-inflammatory Cytokines through Trans-activating Response (TAR) RNA. *J. Biol. Chem.* **291**, 1251–1266 (2016).
11. Dinarello, C. A. Proinflammatory cytokines. *Chest* **118**, 503–508 (2000).
12. DeMarino, C. *et al.* Antiretroviral Drugs Alter the Content of Extracellular Vesicles from HIV-1-Infected Cells. *Sci. Rep.* **8**, (2018).
13. Xu, X., Lai, Y. & Hua, Z.-C. Apoptosis and apoptotic body: disease message and therapeutic target potentials. *Biosci. Rep.* **39**, (2019).
14. Raposo, G. & Stoorvogel, W. Extracellular vesicles: Exosomes, microvesicles, and friends. *J. Cell Biol.* **200**, 373–383 (2013).
15. Tricarico, C., Clancy, J. & D'Souza-Schorey, C. Biology and biogenesis of shed microvesicles. *Small GTPases* **8**, 220–232 (2016).
16. Pleet, M. L. *et al.* Autophagy, EVs, and Infections: A Perfect Question for a Perfect Time. *Front. Cell. Infect. Microbiol.* **8**, (2018).
17. Zhang, Y., Liu, Y., Liu, H. & Tang, W. H. Exosomes: biogenesis, biologic function and clinical potential. *Cell Biosci.* **9**, (2019).
18. Zhang, Q. *et al.* Transfer of Functional Cargo in Exomeres. *Cell Rep.* **27**, 940-954.e6 (2019).

19. Han, L., Lam, E. W.-F. & Sun, Y. Extracellular vesicles in the tumor microenvironment: old stories, but new tales. *Mol. Cancer* **18**, 59 (2019).
20. Guha, D. *et al.* Proteomic analysis of cerebrospinal fluid extracellular vesicles reveals synaptic injury, inflammation, and stress response markers in HIV patients with cognitive impairment. *J. Neuroinflammation* **16**, 254 (2019).
21. Dagur, R. S. *et al.* Neuronal-derived extracellular vesicles are enriched in the brain and serum of HIV-1 transgenic rats. *J. Extracell. Vesicles* **9**, (2019).
22. Chitnis, T. & Weiner, H. L. CNS inflammation and neurodegeneration. *J. Clin. Invest.* **127**, 3577–3587.
23. Petralia, R. S., Wang, Y.-X., Mattson, M. P. & Yao, P. J. Structure, Distribution, and Function of Neuronal/Synaptic Spinules and Related Invaginating Projections. *Neuromolecular Med.* **17**, 211–240 (2015).
24. Bradl, M. & Lassmann, H. Oligodendrocytes: biology and pathology. *Acta Neuropathol. (Berl.)* **119**, 37–53 (2010).
25. Sofroniew, M. V. Astrocyte barriers to neurotoxic inflammation. *Nat. Rev. Neurosci.* **16**, 249–263 (2015).
26. Sofroniew, M. V. Astrogliosis. *Cold Spring Harb. Perspect. Biol.* **7**, (2015).
27. Cohen, J. & Torres, C. Astrocyte senescence: Evidence and significance. *Aging Cell* **18**, (2019).
28. Sonar, S. A. & Lal, G. Differentiation and Transmigration of CD4 T Cells in Neuroinflammation and Autoimmunity. *Front. Immunol.* **8**, 1695 (2017).

29. Clifford, D. B. & Ances, B. M. HIV-Associated Neurocognitive Disorder (HAND). *Lancet Infect. Dis.* **13**, 976–986 (2013).
30. Carroll, A. & Brew, B. HIV-associated neurocognitive disorders: recent advances in pathogenesis, biomarkers, and treatment. *F1000Research* **6**, (2017).
31. Corroon, J. & Kight, R. Regulatory Status of Cannabidiol in the United States: A Perspective. *Cannabis Cannabinoid Res.* **3**, 190–194 (2018).
32. Hosseinzadeh, M., Nikseresht, S., Khodagholi, F., Naderi, N. & Maghsoudi, N. Cannabidiol Post-Treatment Alleviates Rat Epileptic-Related Behaviors and Activates Hippocampal Cell Autophagy Pathway Along with Antioxidant Defense in Chronic Phase of Pilocarpine-Induced Seizure. *J. Mol. Neurosci. MN* **58**, 432–440 (2016).
33. Kosgodage, U. S. *et al.* Cannabidiol (CBD) Is a Novel Inhibitor for Exosome and Microvesicle (EMV) Release in Cancer. *Front. Pharmacol.* **9**, (2018).
34. Kosgodage, U. S. *et al.* Cannabidiol Affects Extracellular Vesicle Release, miR21 and miR126, and Reduces Prohibitin Protein in Glioblastoma Multiforme Cells. *Transl. Oncol.* **12**, 513–522 (2019).
35. Hong, X., Schouest, B. & Xu, H. Effects of exosome on the activation of CD4+ T cells in rhesus macaques: a potential application for HIV latency reactivation. *Sci. Rep.* **7**, 15611 (2017).
36. DeMarino, C. *et al.* Antiretroviral Drugs Alter the Content of Extracellular Vesicles from HIV-1-Infected Cells. *Sci. Rep.* **8**, (2018).

37. Cheli, V. T. *et al.* L-type voltage-operated calcium channels contribute to astrocyte activation In vitro. *Glia* **64**, 1396–1415 (2016).

38. Sofroniew, M. V. Reactive astrocytes in neural repair and protection. *Neurosci. Rev. J. Bringing Neurobiol. Neurol. Psychiatry* **11**, 400–407 (2005).

39. Karimian, A., Ahmadi, Y. & Yousefi, B. Multiple functions of p21 in cell cycle, apoptosis and transcriptional regulation after DNA damage. *DNA Repair* **42**, 63–71 (2016).

40. Stein, G. H., Drullinger, L. F., Soulard, A. & Dulić, V. Differential roles for cyclin-dependent kinase inhibitors p21 and p16 in the mechanisms of senescence and differentiation in human fibroblasts. *Mol. Cell. Biol.* **19**, 2109–2117 (1999).

41. Kang, C. *et al.* The DNA damage response induces inflammation and senescence by inhibiting autophagy of GATA4. *Science* **349**, aaa5612 (2015).

42. Simpson, J. E. *et al.* Population variation in oxidative stress and astrocyte DNA damage in relation to Alzheimer-type pathology in the ageing brain. *Neuropathol. Appl. Neurobiol.* **36**, 25–40 (2010).

43. Sato, Y. *et al.* Diversity of DNA damage response of astrocytes and glioblastoma cell lines with various p53 status to treatment with etoposide and temozolomide. *Cancer Biol. Ther.* **8**, 452–457 (2009).

44. Chen, J.-H., Tsou, T.-C., Chiu, I.-M. & Chou, C.-C. Proliferation Inhibition, DNA Damage, and Cell-Cycle Arrest of Human Astrocytoma Cells after Acrylamide Exposure. *Chem. Res. Toxicol.* **23**, 1449–1458 (2010).

45. Takahashi, A. *et al.* Exosomes maintain cellular homeostasis by excreting harmful DNA from cells. *Nat. Commun.* **8**, 15287 (2017).

46. Schiera, G. *et al.* Oligodendroglioma cells synthesize the differentiation-specific linker histone H1˚ and release it into the extracellular environment through shed vesicles. *Int. J. Oncol.* **43**, 1771–1776 (2013).

47. Burke, M. C., Oei, M. S., Edwards, N. J., Ostrand-Rosenberg, S. & Fenselau, C. Ubiquitinated proteins in exosomes secreted by myeloid-derived suppressor cells. *J. Proteome Res.* **13**, 5965–5972 (2014).

48. Villarreal, L. *et al.* Unconventional Secretion is a Major Contributor of Cancer Cell Line Secretomes. *Mol. Cell. Proteomics MCP* **12**, 1046–1060 (2013).

49. Freund, A., Laberge, R.-M., Demaria, M. & Campisi, J. Lamin B1 loss is a senescence-associated biomarker. *Mol. Biol. Cell* **23**, 2066–2075 (2012).

50. Wang, A. S., Ong, P. F., Chojnowski, A., Clavel, C. & Dreesen, O. Loss of lamin B1 is a biomarker to quantify cellular senescence in photoaged skin. *Sci. Rep.* **7**, 15678 (2017).

51. Shimi, T. *et al.* The role of nuclear lamin B1 in cell proliferation and senescence. *Genes Dev.* **25**, 2579–2593 (2011).

52. Trias, E. *et al.* Emergence of Microglia Bearing Senescence Markers During Paralysis Progression in a Rat Model of Inherited ALS. *Front. Aging Neurosci.* **11**, 42 (2019).

53. Ortiz-Montero, P., Londoño-Vallejo, A. & Vernot, J.-P. Senescence-associated IL-6 and IL-8 cytokines induce a self- and cross-reinforced senescence/inflammatory

milieu strengthening tumorigenic capabilities in the MCF-7 breast cancer cell line. *Cell Commun. Signal. CCS* **15**, (2017).

54. Biran, A. *et al.* Quantitative identification of senescent cells in aging and disease. *Aging Cell* **16**, 661–671 (2017).
55. Shang, D. *et al.* Identification of a pyridine derivative inducing senescence in ovarian cancer cell lines via P21 activation. *Clin. Exp. Pharmacol. Physiol.* **45**, 452–460 (2018).
56. Georgilis, A. *et al.* PTBP1-Mediated Alternative Splicing Regulates the Inflammatory Secretome and the Pro-tumorigenic Effects of Senescent Cells. *Cancer Cell* **34**, 85-102.e9 (2018).
57. Narayanan, A. *et al.* Exosomes derived from HIV-1-infected cells contain trans-activation response element RNA. *J. Biol. Chem.* **288**, 20014–20033 (2013).
58. Bsibsi, M., Ravid, R., Gveric, D. & van Noort, J. M. Broad Expression of Toll-Like Receptors in the Human Central Nervous System. *J. Neuropathol. Exp. Neurol.* **61**, 1013–1021 (2002).
59. El-Hage, N., Podhaizer, E. M., Sturgill, J. & Hauser, K. F. Toll-like receptor expression and activation in astroglia: differential regulation by HIV-1 Tat, gp120, and morphine. *Immunol. Invest.* **40**, 498–522 (2011).
60. Lafon, M., Megret, F., Lafage, M. & Prehaud, C. The innate immune facet of brain. *J. Mol. Neurosci.* **29**, 185–194 (2006).

61. Abulwerdi, F. A. *et al.* Development of Small Molecules with a Non-Canonical Binding Mode to HIV-1 Trans Activation Response (TAR) RNA. *J. Med. Chem.* **59**, 11148–11160 (2016).
62. Feliú, A. *et al.* A Sativex®-like combination of phytocannabinoids as a disease-modifying therapy in a viral model of multiple sclerosis. *Br. J. Pharmacol.* **172**, 3579–3595 (2015).
63. Narayanan, A. *et al.* Exosomes derived from HIV-1-infected cells contain trans-activation response element RNA. *J. Biol. Chem.* **288**, 20014–20033 (2013).
64. Sampey, G. C. *et al.* Exosomes from HIV-1-infected Cells Stimulate Production of Pro-inflammatory Cytokines through Trans-activating Response (TAR) RNA. *J. Biol. Chem.* **291**, 1251–1266 (2016).
65. Sampey, G. C. *et al.* Exosomes and their role in CNS viral infections. *J. Neurovirol.* **20**, 199–208 (2014).
66. DeMarino, C. *et al.* Antiretroviral Drugs Alter the Content of Extracellular Vesicles from HIV-1-Infected Cells. *Sci. Rep.* **8**, 7653 (2018).
67. Pleet, M. L. *et al.* Ebola VP40 in Exosomes Can Cause Immune Cell Dysfunction. *Front. Microbiol.* **7**, 1765 (2016).
68. Pleet, M. L. *et al.* Ebola Virus VP40 Modulates Cell Cycle and Biogenesis of Extracellular Vesicles. *J. Infect. Dis.* (2018) doi:10.1093/infdis/jiy472.
69. Sami Saribas, A. *et al.* HIV-1 Nef is released in extracellular vesicles derived from astrocytes: evidence for Nef-mediated neurotoxicity. *Cell Death Dis.* **8**, e2542 (2017).

70. McNamara, R. P. *et al.* Nef Secretion into Extracellular Vesicles or Exosomes Is Conserved across Human and Simian Immunodeficiency Viruses. *mBio* **9**, (2018).
71. Pužar Dominkuš, P., Ferdin, J., Plemenitaš, A., Peterlin, B. M. & Lenassi, M. Nef is secreted in exosomes from Nef.GFP-expressing and HIV-1-infected human astrocytes. *J. Neurovirol.* **23**, 713–724 (2017).
72. Lee, J.-H. *et al.* HIV-Nef and ADAM17-Containing Plasma Extracellular Vesicles Induce and Correlate with Immune Pathogenesis in Chronic HIV Infection. *EBioMedicine* **6**, 103–113 (2016).
73. Ivey, N. S. *et al.* Association of FAK activation with lentivirus-induced disruption of blood-brain barrier tight junction-associated ZO-1 protein organization. *J. Neurovirol.* **15**, 312–323 (2009).
74. Nakamuta, S. *et al.* Human immunodeficiency virus type 1 gp120-mediated disruption of tight junction proteins by induction of proteasome-mediated degradation of zonula occludens-1 and -2 in human brain microvascular endothelial cells. *J. Neurovirol.* **14**, 186–195 (2008).
75. Song, J. *et al.* Focal MMP-2 and MMP-9 activity at the blood-brain barrier promotes chemokine-induced leukocyte migration. *Cell Rep.* **10**, 1040–1054 (2015).
76. Xu, H. *et al.* The human immunodeficiency virus coat protein gp120 promotes forward trafficking and surface clustering of NMDA receptors in membrane microdomains. *J. Neurosci. Off. J. Soc. Neurosci.* **31**, 17074–17090 (2011).

77. Liu, J., Xu, C., Chen, L., Xu, P. & Xiong, H. Involvement of Kv1.3 and p38 MAPK signaling in HIV-1 glycoprotein 120-induced microglia neurotoxicity. *Cell Death Dis.* **3**, e254 (2012).

78. Chen, Q. *et al.* The P2X7 Receptor Involved in gp120-Induced Cell Injury in BV2 Microglia. *Inflammation* **39**, 1814–1826 (2016).

79. Shrikant, P., Benos, D. J., Tang, L. P. & Benveniste, E. N. HIV glycoprotein 120 enhances intercellular adhesion molecule-1 gene expression in glial cells. Involvement of Janus kinase/signal transducer and activator of transcription and protein kinase C signaling pathways. 9.

80. Ton, H. & Xiong, H. Astrocyte Dysfunctions and HIV-1 Neurotoxicity. *J. AIDS Clin. Res.* **4**, 255 (2013).

81. Bari, M., Rapino, C., Mozetic, P. & Maccarrone, M. The endocannabinoid system in gp120-mediated insults and HIV-associated dementia. *Exp. Neurol.* **224**, 74–84 (2010).

82. Moulard, M., Montagnier, L. & Bahraoui, E. Effects of calcium ions on proteolytic processing of HIV-1 gp160 precursor and on cell fusion. *FEBS Lett.* **338**, 281–284 (1994).

83. Purcell, D. F. & Martin, M. A. Alternative splicing of human immunodeficiency virus type 1 mRNA modulates viral protein expression, replication, and infectivity. *J. Virol.* **67**, 6365–6378 (1993).

84. Hladnik, A. *et al.* Trans-Activation Response Element RNA is Detectable in the Plasma of a Subset of Aviremic HIV-1-Infected Patients. *Acta Chim. Slov.* **64**, 530–536 (2017).

85. Li, Q., Liu, Y. & Sun, M. Autophagy and Alzheimer's Disease. *Cell. Mol. Neurobiol.* **37**, 377–388 (2017).

86. Menzies, F. M. *et al.* Autophagy and Neurodegeneration: Pathogenic Mechanisms and Therapeutic Opportunities. *Neuron* **93**, 1015–1034 (2017).

87. Sittler, A. *et al.* Deregulation of autophagy in postmortem brains of Machado-Joseph disease patients. *Neuropathol. Off. J. Jpn. Soc. Neuropathol.* **38**, 113–124 (2018).

88. Rajendran, L. *et al.* Alzheimer's disease β-amyloid peptides are released in association with exosomes. *Proc. Natl. Acad. Sci.* **103**, 11172–11177 (2006).

89. Emmanouilidou, E. *et al.* Cell-produced alpha-synuclein is secreted in a calcium-dependent manner by exosomes and impacts neuronal survival. *J. Neurosci. Off. J. Soc. Neurosci.* **30**, 6838–6851 (2010).

90. Jy, W. *et al.* Endothelial microparticles (EMP) bind and activate monocytes: elevated EMP-monocyte conjugates in multiple sclerosis. *Front. Biosci. J. Virtual Libr.* **9**, 3137–3144 (2004).

91. Minagar, A. *et al.* Elevated plasma endothelial microparticles in multiple sclerosis. *Neurology* **56**, 1319–1324 (2001).

92. Gomes, C., Keller, S., Altevogt, P. & Costa, J. Evidence for secretion of Cu,Zn superoxide dismutase via exosomes from a cell model of amyotrophic lateral sclerosis. *Neurosci. Lett.* **428**, 43–46 (2007).

93. Basso, M. *et al.* Mutant copper-zinc superoxide dismutase (SOD1) induces protein secretion pathway alterations and exosome release in astrocytes: implications for disease spreading and motor neuron pathology in amyotrophic lateral sclerosis. *J. Biol. Chem.* **288**, 15699–15711 (2013).

94. Fevrier, B. *et al.* Cells release prions in association with exosomes. *Proc. Natl. Acad. Sci. U. S. A.* **101**, 9683–9688 (2004).

95. Chistiakov, D. A. & Chistiakov, A. A. α-Synuclein-carrying extracellular vesicles in Parkinson's disease: deadly transmitters. *Acta Neurol. Belg.* **117**, 43–51 (2017).

96. Dinkins, M. B. *et al.* Neutral Sphingomyelinase-2 Deficiency Ameliorates Alzheimer's Disease Pathology and Improves Cognition in the 5XFAD Mouse. *J. Neurosci. Off. J. Soc. Neurosci.* **36**, 8653–8667 (2016).

97. Winston, C. N. *et al.* Prediction of conversion from mild cognitive impairment to dementia with neuronally derived blood exosome protein profile. *Alzheimers Dement. Diagn. Assess. Dis. Monit.* **3**, 63–72 (2016).

98. Andersson, A. *et al.* Pivotal advance: HMGB1 expression in active lesions of human and experimental multiple sclerosis. *J. Leukoc. Biol.* **84**, 1248–1255 (2008).

99. Sun, Y. *et al.* HMGB1 expression patterns during the progression of experimental autoimmune encephalomyelitis. *J. Neuroimmunol.* **280**, 29–35 (2015).

100. Lo Coco, D., Veglianese, P., Allievi, E. & Bendotti, C. Distribution and cellular localization of high mobility group box protein 1 (HMGB1) in the spinal cord of a transgenic mouse model of ALS. *Neurosci. Lett.* **412**, 73–77 (2007).

101. Ravizza, T. *et al.* High Mobility Group Box 1 is a novel pathogenic factor and a mechanistic biomarker for epilepsy. *Brain. Behav. Immun.* **72**, 14–21 (2018).

102. Festoff, B. W., Sajja, R. K., van Dreden, P. & Cucullo, L. HMGB1 and thrombin mediate the blood-brain barrier dysfunction acting as biomarkers of neuroinflammation and progression to neurodegeneration in Alzheimer's disease. *J. Neuroinflammation* **13**, (2016).

103. Bhakar, A. L. *et al.* Constitutive nuclear factor-kappa B activity is required for central neuron survival. *J. Neurosci. Off. J. Soc. Neurosci.* **22**, 8466–8475 (2002).

104. Koedel, U., Bayerlein, I., Paul, R., Sporer, B. & Pfister, H. W. Pharmacologic Interference with NF-kB Activation Attenuates Central Nervous System Complications in Experimental Pneumococcal Meningitis. 9.

105. Kisseleva, T. *et al.* NF-κB regulation of endothelial cell function during LPS-induced toxemia and cancer. *J. Clin. Invest.* **116**, 2955–2963 (2006).

106. Teng, Z. *et al.* ApoE Influences the Blood-Brain Barrier Through the NF-κB/MMP-9 Pathway After Traumatic Brain Injury. *Sci. Rep.* **7**, (2017).

107. Coelho-Santos, V. *et al.* The TNF-α/NF-κB signaling pathway has a key role in methamphetamine–induced blood–brain barrier dysfunction. *J. Cereb. Blood Flow Metab.* **35**, 1260–1271 (2015).

108. Crescenzi, E. *et al.* NF-κB-dependent cytokine secretion controls Fas expression on chemotherapy-induced premature senescent tumor cells. *Oncogene* **30**, 2707–2717 (2011).

109. Rovillain, E. *et al.* Activation of nuclear factor-kappa B signalling promotes cellular senescence. *Oncogene* **30**, 2356–2366 (2011).

110. Chien, Y. *et al.* Control of the senescence-associated secretory phenotype by NF-κB promotes senescence and enhances chemosensitivity. *Genes Dev.* **25**, 2125–2136 (2011).

111. Walker, D. G., Tang, T. M. & Lue, L.-F. Increased expression of toll-like receptor 3, an anti-viral signaling molecule, and related genes in Alzheimer's disease brains. *Exp. Neurol.* **309**, 91–106 (2018).

112. McKimmie, C. S. & Fazakerley, J. K. In response to pathogens, glial cells dynamically and differentially regulate Toll-like receptor gene expression. *J. Neuroimmunol.* **169**, 116–125 (2005).

BIOGRAPHY

Maria Cowen graduated from Centreville High School, Centreville, Virginia, in 2014. She received her Associates in Applied Science from Northern Virginia Community College in 2017, followed by her Bachelors of Science with a concentration in Biotechnology and Molecular Biology from George Mason University in 2019. She then was accepted into GMU's Accelerated Master's program, allowing her to pursue a Master's of Biology with a concentration in Microbiology and Infectious Disease in 2020. Throughout her undergraduate and graduate college experiences, participating in Dr. Kashanchi's laboratory of Molecular Virology has gained her several skills and experiences such as learning new techniques, participating in academic and professional scientific conferences, and co-authoring several peer-reviewed manuscripts.